PUBLICATIONS

of the

LEANDER McCORMICK OBSERVATORY

of the

UNIVERSITY OF VIRGINIA

Design and Applications of Optical Interferometers in Astronomy

by

Paul H. Knappenberger, Jr.
H. John Wood, III
Laurence W. Fredrick

CHARLOTTESVILLE, VIRGINIA

1966

PUBLICATIONS

of the

LEANDER McCORMICK OBSERVATORY

of the

UNIVERSITY OF VIRGINIA

Design and Applications of Optical Interferometers in Astronomy

by

Paul H. Knappenberger, Jr.
H. John Wood, III
Laurence W. Fredrick

CHARLOTTESVILLE, VIRGINIA

1966

Foreword: This paper is the final report for Grant SC-NGR-47-005-031 from the National Aeronautics and Space Administration. The primary objective of the grant was to test the quality of a telescope under operating conditions. If such tests are valid, then the simple technique of shearing prism tests can surplant the laborious Hartmann tests. A second goal was to study the use of the shearing prism as a collimation tool for reflective telescopes. The enclosed results are disappointing in this aspect (at least 3/5 of our efforts went into this phase of the study) but an alternative is suggested. Finally, the third goal was to have a look at beam interferometers and a brief summary of our studies is given.

A copy of this paper is being forwarded to our Research Grants and Contracts Administrator for the University of Virginia. This completes the grant and he will submit a final fiscal report and see that the unspent funds are returned.

L. W. F.

INTRODUCTION

Interferometry has had a long history in the field of optics and has found many applications in laboratory techniques. In the optical region of the spectrum, stringent requirements on the surface accuracy have demanded very delicate and often cumbersome equipment. As a result, interferometers have found only limited use in the field of Astronomy. Atmospheric and mechanical problems have limited the effectiveness of interferometry in astronomy.

There are three general areas of astronomy in which interferometers find application. The first of these is the testing of optical instruments. After a telescope has been mounted, it is necessary to test the optical system for collimation and performance under actual operating conditions. Tests to determine the types and amounts of aberrations present and the effects of gravitation and temperature gradients on the system are necessary.

The second area involves the measurement of double star separations. The conventional micrometer methods are limited by the resolving power of the telescope, whereas methods of interferometry are effective beyond this limit.

Finally, few reliable measurements of stellar diameters are available. Modern photoelectric techniques should greatly increase our knowledge of stellar diameters when used with optical interferometers. Recent papers have emphasized the need for accurate measurements of stellar diameters (Johnson, 1965) and the work of Michelson and Pease at Mount Wilson must serve only as a beginning.

With the advent of space-age astronomy, the needs for reliable interferometry will increase. The testing of earth-orbit telescopes for de-collimation during launch is one area where interferometry can prove helpful. Development of better techniques and new research into this area must now be undertaken.

Operating under a grant from the National Aeronautics and Space Administration, we have investigated the design and application of interferometers to the three areas of astronomy listed above. Taking each area separately, the results of our investigations are discussed and our recommendations for future study are given.

TESTING OF INSTRUMENTS

Previous methods of testing large telescopes, after they are mounted for use, have been performed with the Foucalt knife edge test or the Hartmann test. These methods have been used for many years and their shortcomings are well known. The Foucalt test does not yield any quantitative results but shows instead the overall quality of the surface being tested. The Hartmann test, which does yield quantitative results of sufficient accuracy, is subject to several other deficiencies. The nature of the screen or mask employed in this technique is such that the test is performed only on various zones. This zonal testing has the serious drawback that a groove or strain line could be situated such that it will not appear in a Hartmann test. A well known example of this occurrence is the 1-meter telescope at the University of Manchester. Kopal (1965) has reported that a groove 8 cm. wide and 0.3λ in depth was not detected in the course of Hartmann testing at the factory due to the "unfortunate distribution of holes in the masks employed for such tests."[1] Furthermore, cumbersome equipment is needed to test a large telescope by the Hartmann technique and much valuable telescope time is taken up. An improved technique for telescope testing is required, and the use of interferometry provides this technique.

We have investigated the methods of testing telescopes interferometrically with the assistance of J. B. Saunders, National Bureau of Standards, Washington, D. C. Mr. Saunders has developed a compact, compound prism which can be used to measure the shape of any converging wave front from any optical element or compound instrument. A detailed description of this prism and the theoretical discussion of wave front shearing interferometry has been given by Saunders (1964). A brief discussion of the theory behind this method follows.

THEORETICAL EXPLANATION OF THE W.S.I.

The prism, shown schematically in Figure (1), is located in the focal plane and on the optical axis of the telescope. The converging beam of light is divided by amplitude division at a semi-reflecting plane extending through the center of the prism. Each of the two components of the beam travel different paths through the prism and is deviated differently by internal reflections so that the two components emerge at a small angle to each other. This angle is called the "angle of shear" and can be varied from prism to prism. Each original ray is divided into four component rays. Two of these rays emerge from each of the two exit faces of the prism. If an observer's eye is placed so as to receive either pair of emerging rays, two images of the objective will be seen. (Primary-

1 Kopal, Z., 1965, Annual Sum. Report No. 3, University of Manchester.

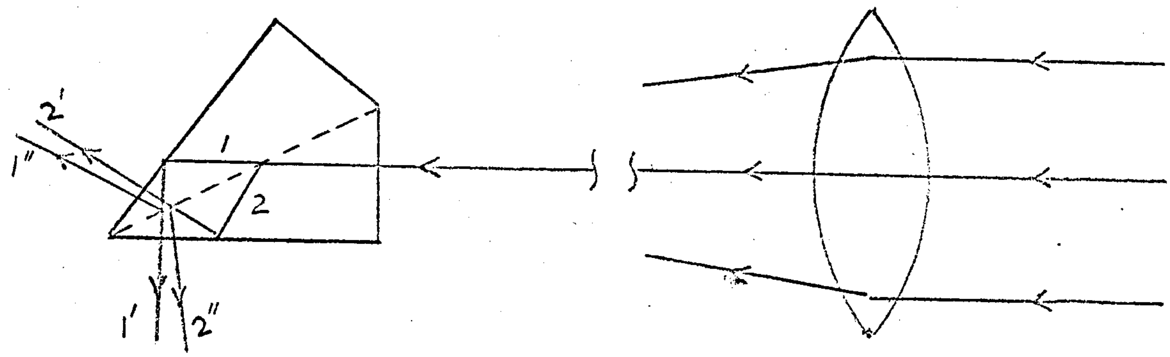

FIG. 1 - The optical diagram of the wave front shearing prism.

secondary mirror combination in case of a reflector). One image will have a slight lateral displacement with respect to the other . Thus, the original wave front has been made to interfere with a sheared image of itself. This interference produces a set of non-localized fringes, whose shape is a function of the shape of the wave front. (A spherical or ideal wave front will produce straight fringes, while an aspherical or aberrated wave front produces curved fringes).

McCORMICK WAVE SHEAR INTERFEROMETER

We have designed and constructed an interferometer housing which permits the prism to be held in the focal plane of a telescope. The instrument mounts in a standard 1-1/4" eyepiece holder and is small enough to fit in one's hand (weight < 3 lbs). A camera is used to receive one of the emerging sets of interference fringes while an eyepiece allows the observer to view the other set of fringes. The design allows an interference filter (or other suitable filter) to be placed in the beam of light, thus, a nearly monochromatic interference pattern is produced. The prisms which are used in our interferometer were constructed by John V. McDermott of the National Bureau of Standards and were donated by him. They are mounted inside a brass tube which slides snugly inside the barrel of the interferometer housing. This arrangement allows us to change prisms at will.

The interferometer was aligned so that the entrance face of the prism is normal to the optical axis of the telescope being tested. A small plano-convex lens has been cemented to the entrance face of the prism, thus, eliminating the need for a camera lens. The interferometer has been calibrated so that both the observer's eye and the camera can be focused on the objective lens of the telescope. This arrangement permits the analysis of the wave front immediately after it emerges from the objective (or mirror). When testing is being performed, a star is used as a point source of light. The star can be centered in the field of view by using an eyepiece with a reticle which can be mounted on the interferometer housing. After the star is focused and centered, this eyepiece can be replaced by a magnification eyepiece which permits the observer to view the fringes.

TESTING THE TELESCOPE

When testing a telescope using this interferometer, the following technique is used. The interferometer is mounted in the eyepiece holder of the telescope and is focused on the objective (or secondary mirror). A suitable prism has been inserted as well as an inteference or absorption filter. A star is chosen to be used as a point source and the necessary exposure time is calculated, using a set of tables prepared by us for this purpose. Exposure times generally vary between 4 seconds and 2 minutes depending on the several factors involved. (Telescope aperature, stellar magnitude, filter, emulsion, sky transparency and focal ratio). The telescope is directed toward the chosen star and using the first eyepiece, the star is focused and centered. After changing eyepieces, the fringes are viewed and centered in the field by slight adjustment of the telescope in hour angle and declination. The zero-th order fringe is centered and the number of fringes in the field is adjusted by sliding the interferometer along the optical axis. The fringe pattern may now be inspected visually and be simultaneously photographed. It is standard procedure to shear the telescopic optics along several diameters, hence the interferometer may be rotated around the optical axis exactly 45°, 90° etc. with respect to the initial position. (This will provide shear along eight equally spaced diameters and permit a rapid and complete analysis of the entire wave front). This entire procedure can be carried out in less than 15 minutes of telescope time, and no modifications need be made to the telescope. The only equipment necessary is the eyepiece interferometer.

REDUCTION OF THE INTERFEROGRAM

The interference pattern which was photographed can be measured and a complete analysis carried out. Saunders (1961) has described a rigorous mathematical operation for interpretation of sheared interferograms that does not depend upon symmetry of wave form. The solution is unique for any chosen family of reference points. This method permits one to evaluate the deviations of the wave front at the chosen reference points from a statistically chosen sphere. The family of reference points must be chosen along a chord parallel to the direction of shear. The fundamental equation in this method can be given as

$$\delta_\nu = \delta_{\nu-1} + q_\nu + r - \nu\varepsilon \quad \nu = 1, 2, \ldots, N \tag{a}$$

The q_ν's represent the deviations of the true wave front from that of the closest fitting sphere. The q_ν's represent the measured order of interference on the interferogram at the chosen reference points. The remaining parameters r and ε are determined in the iteration process. Formula (a) represents N equations in $N + 3$ unknowns. (namely, $(N + 1)$ δ_ν's, r and ε).

However, the δ_{ν}'s do not have significance until the reference circle is defined. The circle of reference may be fully defined by three equations of condition and when these are combined with the set of observation equations, data from a single set of fringes is sufficient for a complete solution. With some slight modifications, the Saunders procedure has been programmed for calculation on a digital computer. The reference circle is chosen using the method of least squares and the only data necessary are the values of the q_{ν}'s as measured on the interferogram. The computer requires less than a minute to compile and compute the desired deviations. An analysis of the wavefront along eight different diameters requires measurement of eight interferograms with one family of reference points plotted on each. The technique of measurement is simple and requires only a small amount of time.

The results of the tests may be displayed in tabular form or plotted graphically. Both of these methods are used in this paper to present the results of several tests. Another method of displaying the results is to form a type of contour diagram which indicates the shape of the entire wave front.

Several telescopes have been tested using this technique of interferometry. The 26-inch Leander McCormick refractor was tested by both Saunders and Knappenberger. Saunders (1964) has published the results of his tests and the more recent tests by Knappenberger using a different prism have confirmed Saunders' results. This report includes the first application of this technique to the testing of large astronomical reflectors. The 32-inch reflector at the Fan Mountain Observing Station of Leander McCormick Observatory has been tested repeatedly under various test conditions. This telescope is frequently tested under various conditions of temperature, position angle, mirror-mounting tensions, and misalignment. The 24-inch reflector at Mt. Cuba Observatory in Delaware was also tested this summer.

As a thorough test for the interferometry method, we had the opportunity to test the 84-inch reflector at Kitt Peak National Observatory while Hartmann tests on this same instrument were being carried out. The details of the tests of these three instruments are described below.

32-INCH FAN MOUNTAIN REFLECTOR

The 32-inch reflector at Fan Mountain Station of Leander McCormick Observatory is the first reflector to have been tested by this technique. The Cassegrain reflector has an effective focal ratio of f/16 when in normal use, but interchangeable secondary mirrors permit the use of an f/32 beam. Series of tests have been performed on this telescope under various test conditions. The effects of gravity at different position angles and temperature gradient effects have been studied. The most noticeable change in the shape of the wave front is produced by the tensions due to the mirror mounting. The results included in this paper point out this effect.

The first set of data was taken on the night of May 26, 1965. The star used for a light source was Arcturus and the sky transparencey was rated 3^- on a scale of 4 maximum. The fringe pattern was photographed through interference filter B and the exposure times were about 20 seconds per exposure. Several photographs were made at the following settings: shear NS, EW, SN and WE. The best photographs in each shear direction were chosen and the data was reduced. The results are shown graphically in Plots 1 and 2. (See Appendix B for tables and plots of McCormick telescope). Plot 1 depicts the deviations of the true wave front from a close fitting sphere (chosen by a least squares solution), along the north-south diameter of the mirror combination. Each point on the graph represents the average of three points corresponding to three separate interferograms. The size of the arrow indicates the size of the probable error in positioning of this point. Plot 2 represents deviations along the east-west diameter.

The end points of the mirror and the points closest to the center hole show generally the largest deviations. This can be caused by several separate conditions. First, the edges of the mirror are often very slightly turned either up or down in the grinding and polishing processes. Secondly, the support system which utilizes three support bands around the edge of the mirror could cause a slight turning near the edges. Finally, the technique for measuring the order of interference at the end points and points closest to the central hole is necessarily less accurate than for the other reference points. Hence, the end points have the largest probable error and would be expected to exhibit some turning. Since a close fitting sphere is determined by the method of least squares, any points with large deviations will cause the deviations of the other points to be somewhat larger. The plots show that the mirror combination produces a wave front with definite aberrations present and these aberrations cause deviations of as much as 0.3λ at some points. It should be mentioned that the 26-inch refractor at Leander McCormick Observatory has exhibited the best wave front tested so far. The total deviations of this objective are less than a quarter wave.

To illustrate the effects of tension on the mirror, some results have been included which show the shape of the wave front of the same 32-inch reflector after the tension in the mounting straps has been altered. The second set of McCormick plots (3, 4, 5, 6) were made from data taken on the night of August 12, 1965. Several days prior to this, some adjustment was made to the three support straps surrounding the primary mirror. Several exposures were taken along each of eight diameters and the best of these were used to obtain the plots shown. Vega was the light source and a yellow absorption filter was used. Comparison of the plots before and after the changed tension shows the effect on the wave front. The tightening of the bands produced a slight strain in the primary mirror which showed up in the fringe pattern.

It is possible to visually detect the strain being placed on a mirror by its mounting cell by inspection of the fringe pattern. This technique should prove very useful when testing telescopes at the time they are mounted. By visually inspecting the fringe pattern one can achieve the best possible adjustment of the mounting cell and support system. A photograph of the fringe pattern taken on May 26, 1965 is shown in Figure 2.

MT. CUBA 24-INCH REFLECTOR

The second reflector tested using this technique was the new 24-inch Cassegrain reflector at Mt. Cuba Observatory, near Wilmington, Delaware. This telescope was tested on only one night, August 3, 1965 with the assistance of Dr. R. B. Herr, University of Delaware. The star Vega was used as a light source and interference filter B (see Appendix A for list of filters) was inserted in the light beam. The sky transparency was rated very good but the seeing was not perfect. Exposures were taken along eight

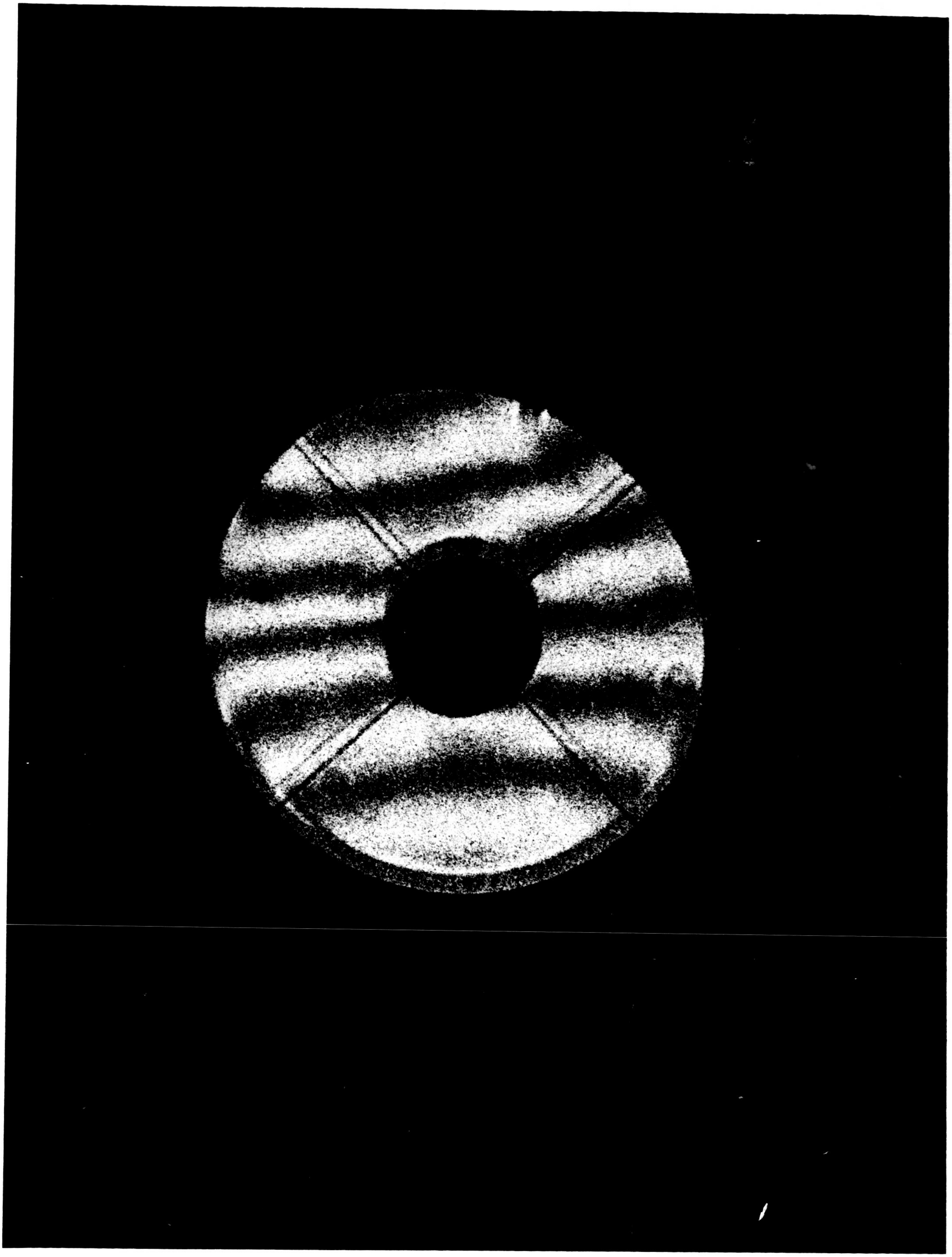

FIG. 2 - Interferogram of the 32-inch McCormick reflector.

diameters but only the best photographs were chosen to compute the shape of the wave front, and these had directions of shear either north-south or east-west. The data was analyzed and the results are shown in plots 7 and 8 (Appendix C). Once again the end points exhibit the largest deviations as expected. More nights of testing would be required to yield a complete analysis of the mirror system. The telescope would have to be tested along the eight diameters at various temperatures and at different zenith angles. Improvements in the shape of the wave front could be obtained by small adjustments to the support system. Preliminary adjustments could be easily carried out by changing the mounting cell tensions and checking visually, the shape of the fringe pattern.

KITT PEAK 84-INCH REFLECTOR

A comparison between the interferometry technique and the well-known Hartmann technique seemed highly desirable, and when the opportunity arose to compare results from the two techniques applied to a very large reflector, this task was undertaken. For three nights in succession, September 8, 9, 10, 1965, the 84-inch reflector at Kitt Peak National Observatory was tested at the Cassegrain focus. With the assistance of Dr. A. Hoag, independent tests were performed by Saunders and Knappenberger. Each observer used his own set of prisms and filters and his own interferometer housing. The reduction of the interferograms was carried out independently by each observer and at the time of this writing, a preliminaty check has indicated close agreement. The following is a description and results of the tests by Knappenberger.

On September 8, 1965 the sky was partially cloudy and both the seeing and transparency conditions were only fair. α Aql. was used as the light source and several exposures along various diameters were made. None of these photographs were used in the results shown in this paper. On September 9, 1965 the conditions were considerably better and Vega was used as the light source. Exposures of 3 seconds were made at each of eight diameter settings through the yellow absorption filter. Eight of these photographs were used and the results were combined with the photographs taken the next evening. On the 10th, the seeing was good and the transparency excellent and again Vega was used. It should be noted that Vega was almost on the meridian during the testing period. The fringes were photographed through interference filter B and the exposure time was 5 seconds. Figure 3 shows a photograph of the fringe pattern taken on September 10, 1965.

The interferograms were measured and reduced at the University of Virginia. The results are shown in plots (9, 10, 11, 12) in Appendix D. The arrow in the upper left hand corner of each plot indicates the size of the probable error. The end points and the points near the center of the mirror have been omitted because of the great uncertainty in reading the order of interference at these points. The plots reveal high and low zones on the mirror as well as slightly turned edges. Examination of the interferograms shows many small zones near the outer edge of the mirror. These small zones require several families of reference points to be measured in order to bring these out in the plot. Nevertheless, it is interesting to note the zones and compare the interferograms with Foucalt knife tests of the same mirror. When this is done, it can be seen that the shadows of zones in the Foucalt test correspond exactly with the "blips" on the fringes. This result could not be ascertained using the Hartmann technique.

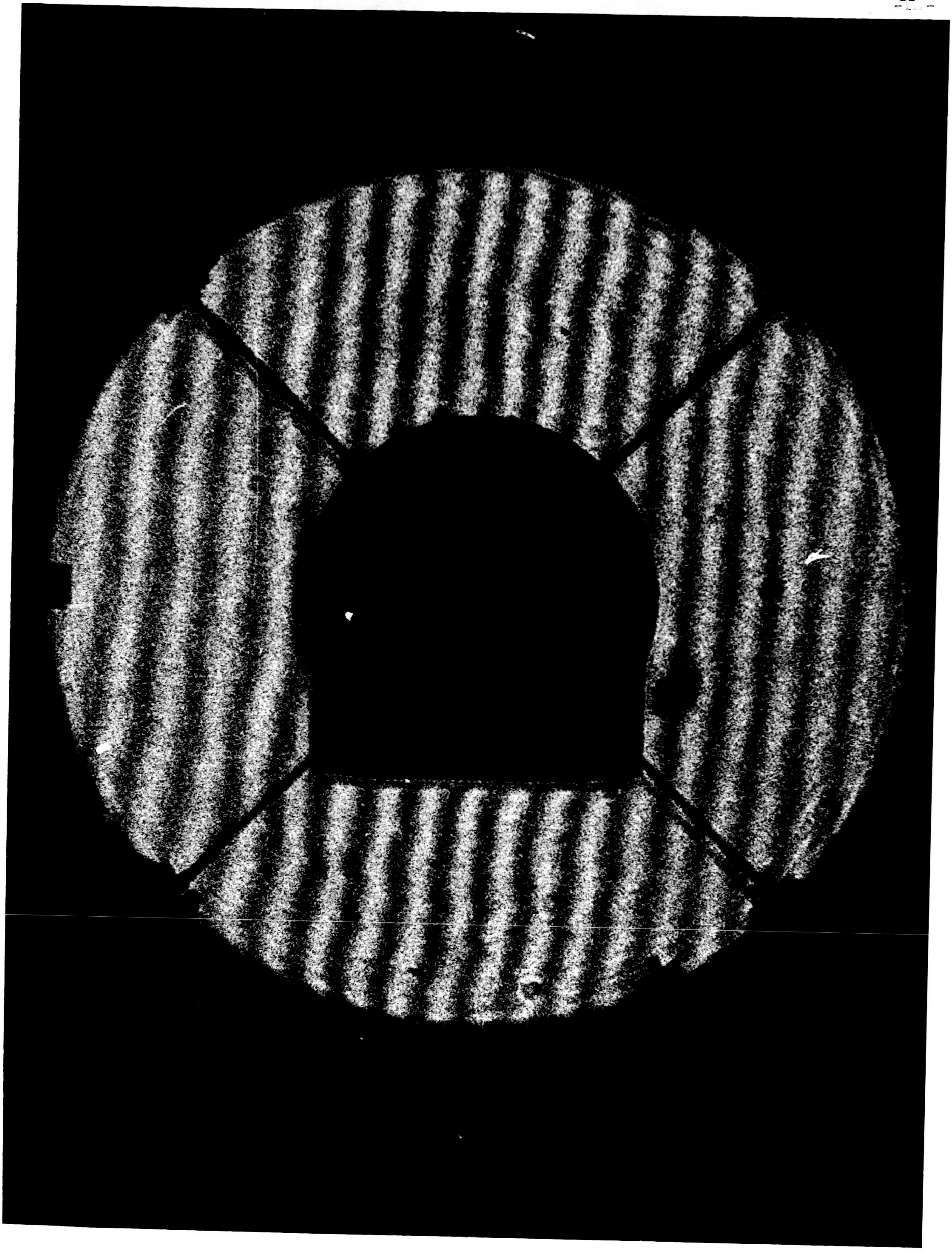

FIG. 3 - Interferogram of the 84 - inch Kitt Peak reflector.

As was mentioned previously, a comparison between the Hartmann technique and the interferometry method is desired. Hartmann tests were performed on the 84-inch reflector on the nights immediately preceding the interferometer tests. The results of the Hartmann tests were made available to us by Kitt Peak in late January, 1966. Hence, only a preliminary check between the Hartmann results and the interferometer results could be made.

It was found that the overall shape of the wave front determined by both tests agreed reasonably well; however, the interferometer tests indicated zones and turned edges which were not shown by the Hartmann test.

A more complete comparison between the two tests will be carried out and the results of these tests will probably be published jointly with Kitt Peak.

SEPARATION OF ABERRATIONS

It would be useful if one could obtain the coefficients of the Seidel aberrations from the results of the interferometer tests. R. Kingslake (1926) has described a method of analyzing the interferometer pattern produced by a lens, in order to obtain a measure of the aberrations. We consider the equations used for evaluating the fringe pattern produced by the wave front shearing interferometer. Referring to Fig. (4) we can write $\delta_{\dot{x}} + s_{\dot{x}} = q_x + \delta_x - 1$. As was shown by Saunders (1961) we can write $Sx = (\mu - x)\varepsilon$ and finally

$$\delta_x = \delta_{x-1} + q_x + r - x\varepsilon \tag{1}$$

where x = distance along C from the center of the objective to the reference point, μ = distance along C from the center of the objective

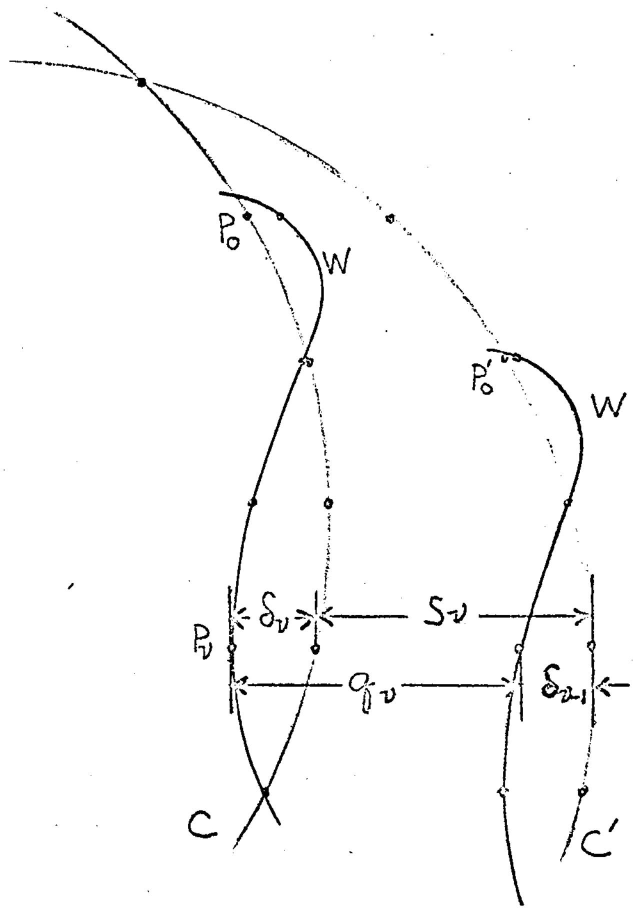

FIG. 4 - Illustration of the two wave fronts relative to the images of a reference sphere.

to the intersection of C and C',

$r = \mu\varepsilon$,

q_x = the order of interference at the point Px,

δx = deviation of true wave front from close fitting sphere.

If we shear along two axes perpendicular to each other and choose one axis as the x-axis and the other as the y-axis, then we can write

$$\delta_x = \delta_{x-1} + q_x + r_1 - x\varepsilon_1 \qquad (1a)$$

$$\delta_y = \delta_{y-1} + q_y + r_2 - y\varepsilon_2 \qquad (1b)$$

Kingslake (1925) has taken A. E. Conrady's equation for optical path difference and modified it to evaluate the primary aberrations of lenses with a Twyman interferometer. By deleting the coefficients which relate to the adjustments of the Twyman interferometer, we can write the formula for optical path difference as

$$A(x^2 + y^2)^2 + By(x^2 + y^2) + C(x^2 + 3y^2) + G = P \qquad (2)$$

where A, B, C represent, respectively, coefficients of spherical aberration, coma and astigmatism. These coefficients are related to the Seidel aberration constants by the equations,

$$4A = a_1 = \frac{\text{Longitudinal (primary) spherical Aberration}}{s^2\, f^2}$$

$$\frac{fB}{h} = a_2 = \frac{\text{coma}}{s^2 h} \qquad (3)$$

$$\frac{2f^2C}{h^2} = a_3 = \frac{\text{distance between focal lines}}{2h^2}$$

where S is the semi-aperture of the lens, h is the image distance from the optical axis and f is the focal length. The order of interference is G at the origin (on the axis of the lens) and is P at any point (x, y).

Now, on the x-axis, we can write eq. (2) as

$$\delta_x = Ax^4 + Cx^2 + G \tag{4}$$

and along the y-axis

$$\delta_y = Ay^4 + By^3 + Cy^2 + G. \tag{5}$$

Combining eqs. (1a) and (4) and after rearranging the terms we obtain

$$A(2x - 1)(2x^2 - 2x + 1) + C(2x - 1) - q_x - r_1 - \varepsilon_1 x = 0. \tag{6}$$

Eq. (6) is not exact, however, since error does exist in the measured value of q_x. If the error is Δq_x then eq. (6) can be rewritten as

$$A(2x - 1)(2x^2 - 2x + 1) + C(2x - 1) - q_x - r_1 - \varepsilon_1 x = \Delta q_x. \tag{7}$$

If we assume that the lens is afflicted with first order aberrations only and that A, B, and C are constant over the entire lens, and if we impose the condition that the sum of the $\Delta q_x 2$ is to be a minimum then we can find a method for evaluating the Seidel aberrations.

First, let

$$\Sigma \Delta q_x^2 = \Sigma \left[A(2x - 1)(2x^2 - 2x + 1) + C(2x - 1) - q_x - r_1 - \varepsilon_1 x\right]^2 = \Sigma M^2.$$

Now,

$$\frac{\partial \Sigma \Delta q_x^2}{\partial A} = \frac{\partial \Sigma M^2}{\partial A} = 2\Sigma(2x - 1)(2x^2 - 2x + 1)\, M = 0$$

$$\frac{\partial \Sigma \Delta q_x^2}{\partial C} = \frac{\partial \Sigma M^2}{\partial C} = 2\Sigma(2x - 1)\, M = 0$$

$$\frac{\partial \Sigma \Delta q_x^2}{\partial \varepsilon_1} = \frac{\partial \Sigma M^2}{\partial \varepsilon_1} = 2\Sigma(-x)\, M = 0$$

$$\frac{\partial \Sigma \Delta q_x^2}{\partial r_1} = \frac{\partial \Sigma M^2}{\partial r_1} = 2\Sigma(-1)\, M = 0$$

and upon substitution for M and rearrangement of the terms we arrive at

$$A\Sigma\left[(2x-1)^2(2x^2-2x+1)^2\right] + C\,\Sigma\left[(2x-1)^2(2x^2-2x+1)\right]$$
$$-r_1\Sigma\left[(2x-1)(2x^2-2x+1)\right] - \varepsilon_1\Sigma\left[x(2x-1)(2x^2-2x+1)\right] =$$
$$\Sigma\left[q_x(2x-1)(2x^2-2x+1)\right]$$
$$A\Sigma\left[(2x-1)^2(2x^2-2x+1)\right] + C\Sigma(2x-1)^2$$
$$-r_1\Sigma(2x-1) - \varepsilon_1\Sigma x(2x-1) = \Sigma\, q_x(2x-1) \qquad (8)$$
$$A\Sigma\left[-x(2x-1)(2x^2+1)\right] + C\Sigma(-x)(2x-1)$$
$$-r_1\Sigma(-x) - \varepsilon_1\Sigma x(1-x) = \Sigma\, q_x(-x)$$
$$A\Sigma\left[(2x-1)(2x^2-2x+1)\right] + C\Sigma(2x-1) - r_1(n-1) - \varepsilon_1\Sigma x = \Sigma q_x$$

where N = number of reference points.

If a similar procedure is applied to the equations along the y axis, then a set of equations (8') corresponding to (8) will be obtained. Solution of the four simultaneous equations in set (8) and the five simultaneous equations in set (8') will yield numerical values for A, B, and C.

We have just described a method for obtaining values for the Seidel coefficients of spherical aberration, astigmatism and coma using the data from the wave front shearing interferometer. It should be possible to obtain a measure of the quality of a lens or mirror by testing it with the wave front shearing interferometer.

COLLIMATION TECHNIQUES

An attempt to use the wave front shearing interferometer to measure decollimation effects in a Cassegrain reflector was carried out at the McCormick Observatory. Since a misalignment in the optics causes a non-symmetrical distortion in the deviated wave front, it was supposed that the WSI would prove very useful in evaluating decollimation effects. In order to test this statement, an 8-inch Cassegrain reflector located at the Leander McCormick Observatory was modified for the purpose. An attachment for the secondary mirror support was designed which would enable the secondary mirror to be tilted off-axis with respect to the optical axis of the primary. The modification would allow the tilted secondary to be rotated about the optical axis of the primary, thus permitting a controlled amount of tilt in any direction. The angular amount of tilt was controlled by a finely threaded rod which extended out beyond the telescope tube and the adjustments could be made quite easily by a single observer.

The modifications were carried out in the machine shop of the Department of Astronomy by the instrument maker, Hermann Bluemel. Once completed, the telescope was remounted and the testing was started. It was hoped that any decollimation effects could be detected quite readily by significant changes in the fringe pattern. However, this was not the case. Only by tilting the secondary mirror through large angles ($\sim 5°$) could any noticeable change in the fringe pattern be detected. Very small decollimation effects could not be detected by visually examining the fringes. Only after measurement of the interferogram and subsequent reduction of the data did the effects become evident.

As is evident from the theory of wave front shearing interferometry, the interferometer does not compare the wave front being tested with reference sphere, but rather compares the wave front with a sheared image of itself. The shape and the width of the fringes are measures of the deviation of the original wave front from a sphere. If the angle of shear is small (about 0.0039 radians or less), the curvature and difference in width of the fringes is also small for slight deviations of the wave front from the sphere. The larger the shear angle, the more noticeable becomes the curvature of the fringes and the accuracy in testing becomes correspondingly higher. It should also be mentioned that the wave front shear prism can be constructed with a built-in wedge which allows the fringes to rotate. The fringes can therefore be rotated so as to be parallel to the direction of shear. Keeping these points in mind, let us consider the problem of the decollimation of a Cassegrain reflector.

The tilting of the secondary mirror causes the optical axis of the secondary mirror to make a small angle with the optical axis of the primary mirror. Thus, a converging spherical wave front produced by the primary mirror will, upon encountering the secondary, be given a certain non-symmetrical distortion. The amount of distortion will depend upon the size of the angle between the optical axis of the secondary and primary mirrors. If the tilt is small, the amount of distortion will be small. Now, if the slightly distorted wave front were compared with a reference surface (either an optical flat or a reference sphere) the discrepencies in the resulting fringe pattern could be easily noticed. However, if the wave front were given only a small amount of shear and caused to interfere with itself, the discrepencies would not be easily recognized. This statement has been confirmed by our testing with prisms of small shear. It would seem that if one used a prism with a large shear angle, say 0.0060 radians or greater, the effects would be more pronounced. However, we did not have such a prism readily available.

Another point worth mentioning is that the prisms which we used in these tests did not have a built-in wedge. In this case, the fringes remain always perpendicular to the direction of shear and the width (or spacing) of the fringes determines the shape of the wave front. It would be a much simpler task to detect deviations from a straight line along one fringe than to detect small changes in the width of the fringes across the fringe pattern. It would appear then, that if the wave front shearing interferometer were to be used to test Cassegrain reflectors for decollimation, a prism with a built-in wedge and a large shear angle would be required. In discussing this problem with Mr. Saunders of the National Bureau of Standards, it was brought to our attention that the Kösters prism, as modified by Saunders, would be the ideal prism to use for such a task.

The Kösters prism will be discussed in some detail later in this paper in connection with double star and stellar diameter work. It is sufficient here to point out that this prism folds one-half of the wave front being tested over onto the other half. Therefore, any non-symmetries in the wave front become immediately obvious. This prism is extremely sensitive to non-symmetry of wave form and this property makes the Kösters prism ideally suited for our desired tests for decollimation. We propose to obtain a Kösters prism as well as a shearing prism with built-in wedge and large shear angle and use both of these prisms to test our modified reflector for decollimation effects. It should be possible to visually align a Cassegrain reflector using these prisms, and we propose a thorough test of this statement. A catalogue of interference patterns could then be produced under all conditions of misalignment which would be most useful to astronomers when aligning a two element or more reflector. Since, these prisms are so small but yet so rugged, they could easily be used to test for decollimation in earth orbit telescopes. The forces encountered during launch would tend to introduce some decollimation into a reflector type system. By transmitting the fringe pattern produced by one of these prisms back to earth, a check with a catalogue of fringe patterns would enable the observer to make a correction in the proper direction by the proper amount. Further investigations into this technique are therefore needed.

The first area of astronomy in which interferometers find application has just been discussed. This area of testing of instruments can be greatly improved by using techniques of interferometry. Methods of testing telescopes interferometrically have been described and the results that can be expected have been shown. Wave front shearing prism techniques offer many improvements over presently existing methods of testing. Visual inspection of fringe patterns permits adjustments to be made to the support system of a mirror, while careful analysis of the interferogram yields the Seidel coefficients of the primary aberrations in an optical system. The small size of the test instrument and the ease with which it can be used are very favorable characteristics. We now turn our attention to the second area of astronomy in which interferometry finds application.

DOUBLE STAR TECHNIQUES

Conventional methods of measuring double star separations are limited by the resolving power of the telescope. In order to set the micrometer cross hairs on the two stars, they must be resolved. The formula for the resolving power of a telescope is

$$d'' = \frac{1.22\lambda}{A} \times 206265''.$$

Here d is the separation in seconds of arc between two stars which can just be resolved, A is the telescope aperture and λ is the wavelength expressed in the same units as A. This theoretical limit is never reached, however, due to seeing conditions. The use of interferometry techniques enables one to work below the limit set by the resolving power. The Kösters prism provides such a technique and it is discussed below.

THE KÖSTERS INTERFEROMETER

Details on the construction and alignment of a Kösters double-image prism and a discussion of the Kösters interferometer and its various applications have been given by J. B. Saunders (1957a, 1957b). In a more recent publication, Saunders (1963) describes how the Kösters prism can be used as an alignment interferometer and points out that the prism is extremely sensitive to position of the source. A brief description of the Kösters prism will aid in understanding the discussion which is to follow.

The Kösters prism is made by cementing two identical right-angled prisms back to back, with their common surface being aluminized to act as a beam divider. The entrance face can be ground to a spherical shape to reduce refraction effects when a converging light beam is being used. A thin cement wedge is formed between the two components of the prism and all adjustments are carried out before the cement is hardened. If the Kösters prism is placed near the focal point of a telescope and the beam dividing plane is adjusted so as to coincide with a diameter of the telescope lens or mirror, then the observer will see an image similar to that shown in Fig. 5(b). The prism folds one-half of the wave front over onto the other half and introduces some tilt between the two halves. If a point

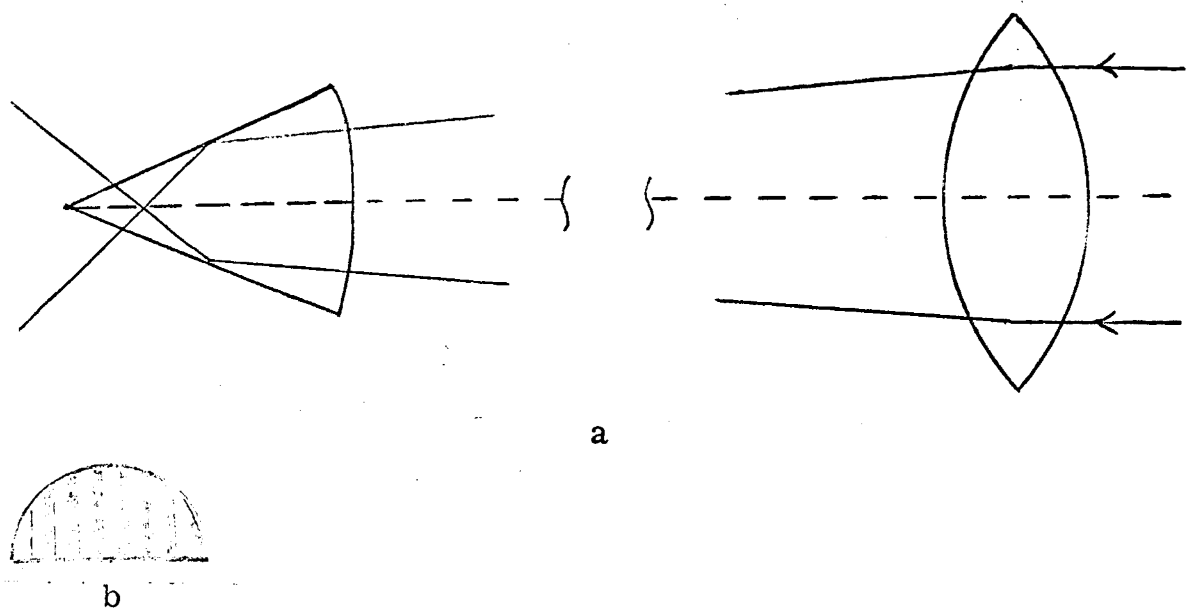

FIG. 5 - (a) The optical diagram of the modified Kösters prism.
5 - (b) Interference pattern produced by Kösters prism.

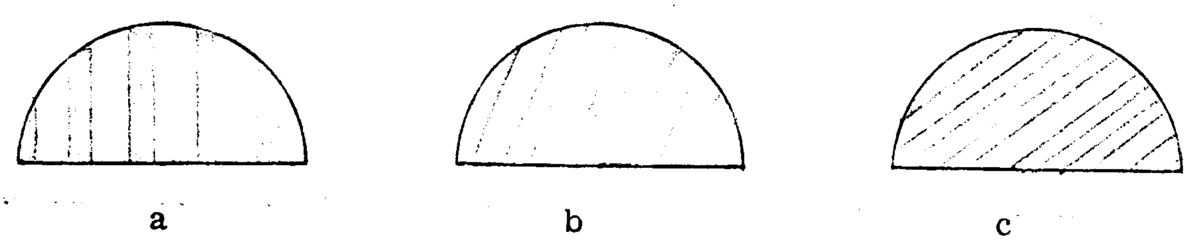

FIG. 6 - The appearance of the interference fringes when the point source is (a) in the beam divider plane, (b) off of the plane, (c) further off the plane.

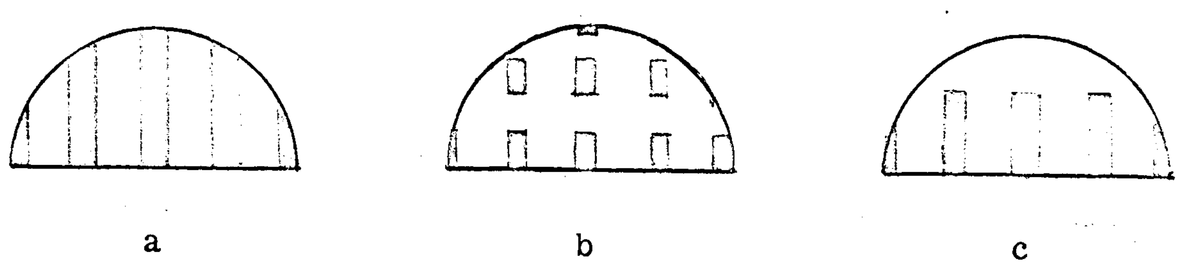

FIG. 7- The appearance of the interference fringes when the source is (a) single, (b) double, (c) extended

source is used and lies in the plane of the beam divider, the fringes will be perpendicular to the dividing plane. If the source is moved off of the plane of the beam divider, the fringes will remain fixed at the dividing plane but the angle between the fringes and the dividing plane will be altered. Figure 6 shows this effect.

In the case of a double source, each point source will produce its own set of interference fringes. These two sets of interference fringes will have a definite angle between them, dependent upon their separation The resulting pattern will be a series of bright and dark bands parallel to the dividing plane. These bands will be produced by the fade out and support of the two sets of fringes.

The separation between adjacent dark bands (nulls) or adjacent bright bands is inversely proportional to the separation of the stars. The equation showing this relationship is given as

$$d'' = \frac{\lambda}{4S} \times 206265'' \tag{10}$$

where d is the angular separation between the stars, λ the wavelength being used and S is the distance from the dividing palne to the first fade-out. The limiting case occurs when the first fade-out is at the edge of the objective farthest from the dividing plane. In this situation, S/2 and hence the limiting separation which can be measured is given by

$$d''_{(lim)} = \frac{\lambda}{2A} \times 206265''. \tag{11}$$

This limit is below the resolving power of the telescope and separations one-half as small as the resolving limit of the telescope can theoretically be measured. With atmospheric seeing, the fringes will wave like the stripes on a flag but they remain anchored at the dividing plane and the bright and dark bands will not be shifted. Unless the atmospheric turbulence becomes too great, the fade out distance can readily be measured. This interferometer is similar to the wave front folding stellar interferometer described by L. Mertz (1963) but permits measurement of fainter stars.

Saunders has constructed an eyepiece attachment that holds a Kösters prism in the correct position near the focal plane and permits adjustment of the orientation of the beam dividing plane. This instrument has been tested briefly on the Leander McCormick 26-inch refractor and appears to be very promising. A small micrometer in the viewing eyepiece permits measurements on the first fade-out to be made. The position angle is determined by rotating the beam divider plane and measuring the first fade-out. When the beam dividing plane is coincident with the line joining the two stars, the two sets of fringes will be coincident and no fade-out will occur, and when the beam divider plane is perpendicular to the line joining the two components, the fade-out distance will be a minimum.

Unlike many interferometers currently being used to measure double star separations, this technique utilizes the whole telescope objective, rather than only two small slits. Thus, the limiting magnitude which can be reached by this method should be somewhat greater than that reached by other techniques. This same principle can be applied to stellar diameter measurements and this is discussed in the next section.

STELLAR DIAMETER MEASUREMENTS

The Michelson stellar interferometer has been used by various observers in attempts to measure stellar diameters. The original work, which was done by Michelson and Pease at Mt. Wilson Observatory, produced the apparent angular size of about seven stars, all of them giants or supergiants of late spectral type. A later attempt by Pease, using a 50 ft. interferometer beam, turned out to be somewhat fruitless. The mechanical rigidity of the interferometer beam was not sufficient enough to prevent optical path differences from being introduced into the two channels of the interferometer. Another serious problem was that the outer mirrors had to be adjusted until the fringe visibility was a minimum in order to get an estimate of the stellar diameter. During this procedure, path inequalities were introduced which caused even the fringes of the comparison star to disappear.

The effects of atmospheric seeing seriously reduced the reliability of the quantitative results obtained. As was pointed out in a recent discussion with Dr. Willet Beavers of Iowa State University, even at six feet separation there is a definite coherence loss, probably due to atmospheric scintillations. This has the effect of reducing the visibility of the fringes and could cause the fringes to disappear before the star was resolved.

We have made a careful study of the Michelson stellar interferometer and the application of modern electronic and recording techniques to it. We have discussed the problem in some detail with Dr. Willet Beavers, who is currently engaged in Michelson interferometer work at Iowa State University, Ames, Iowa. Dr. Beavers is using the Michelson technique and applying electronic detectors and recorders. Figure 8 shows the principle of Dr. Beavers' instrument. Two rectangular mirrors (M_1M_2) about 1" by 6" effective aperture are used to gather the light and reflect it to the image forming mirror M_3. The fringes are detected photoelectrically and the visibility of the fringes can be measured quantitatively, hence there is no need to extend the beam to the separations where the visibility is a

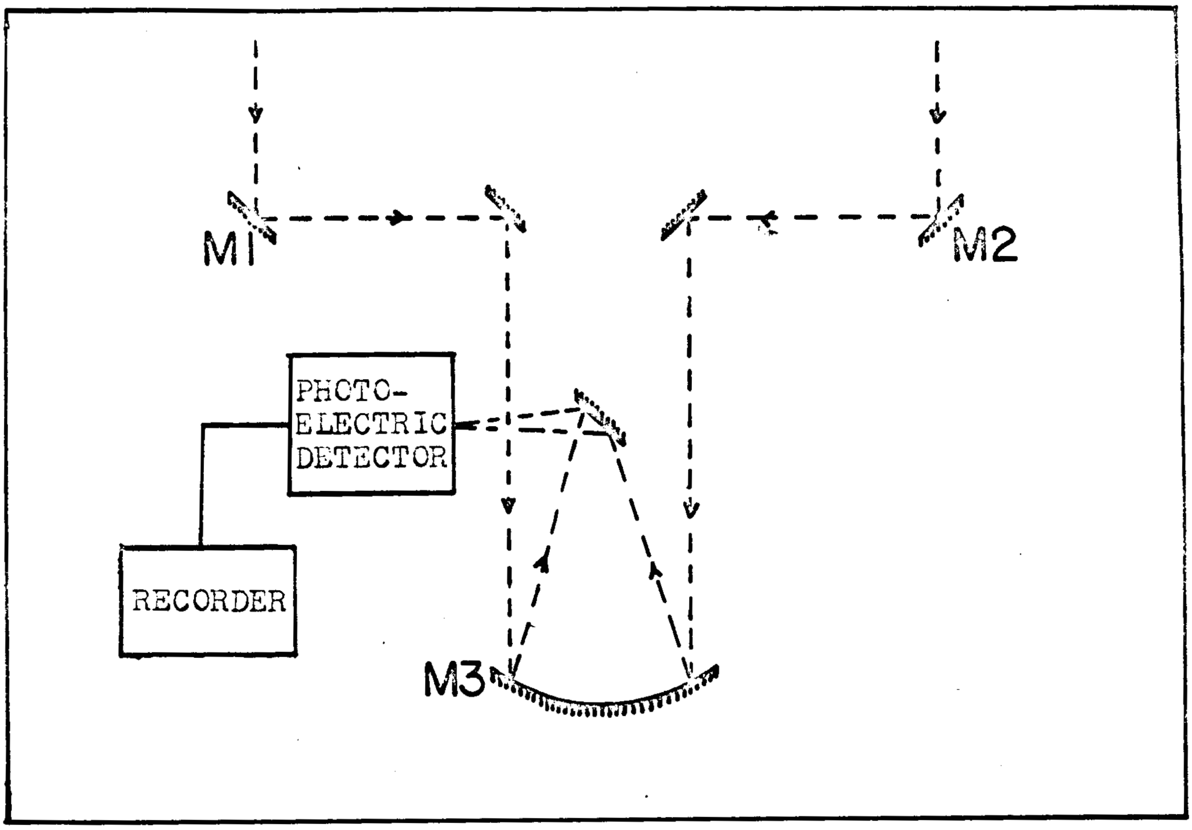

FIG. 8 - The optical diagram for a Michelson stellar interferometer showing Dr. Beavers' electronic additions.

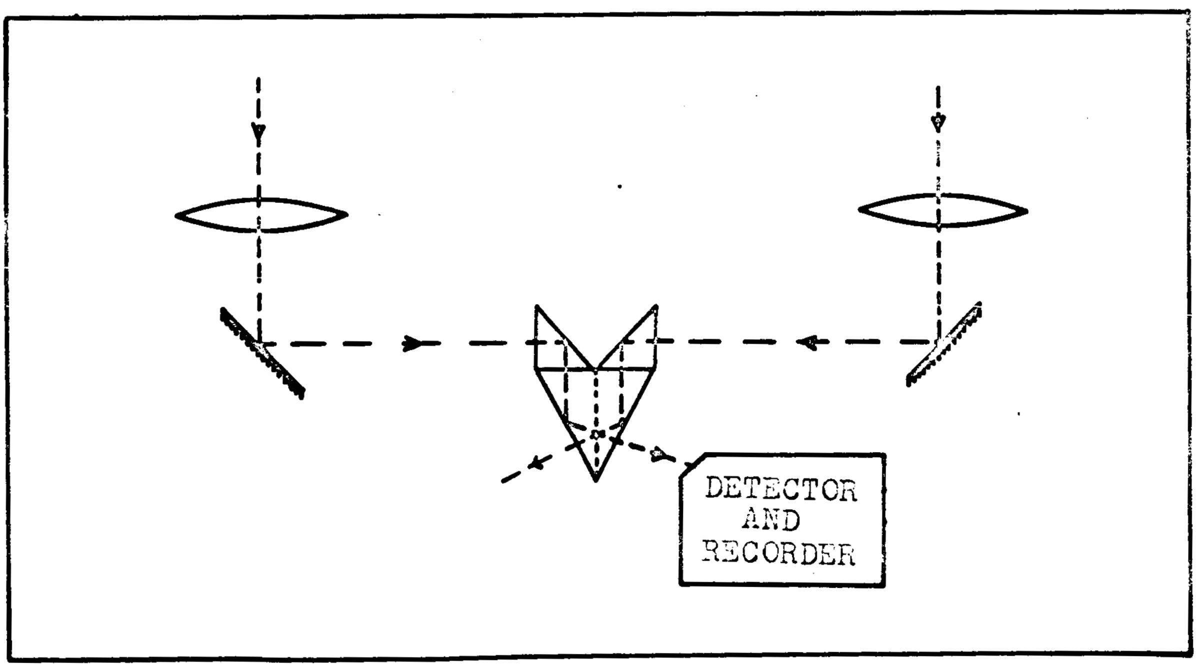

FIG. 9 - The optical diagram for the proposed stellar interferometer using the modified Kösters prism.

minimum. Dr. Beavers believes that such measurements would reduce the mirror separation needed to measure any given angle by at least a factor of 4 and it would be possible to measure limb darkening of a number of stars. It will be necessary to measure the relationship between scintillation effects and the fringe visibility, and take this coherence loss into account when determining the actual fringe visibility at a given mirror separation.

The observations by Michelson and Pease were done visually and the best they could do was to estimate the coherence loss due to atmospheric scintillation. Furthermore, since they were working at separations where the fringe visibility curve was a minimum, the assumptions they made on limb darkening could affect the angular diameter of a star to a large extent. The use of photoelectric detection techniques permits one to measure the coherence loss quite accuarately and make the necessary corrections for it. The technique also permits one to work further in on the visibility curve where the effects of limb darkening are not as great.

We have examined the possibility of using the Kösters prism as a stellar interferometer and have concluded that there are very definite advantages in this technique. With some slight modifications to Figure C-2d found in Saunders contribution to John Strong's <u>Concepts of Classical Optics</u>, (1958), the optical diagram of the interferometer that we have studied is shown in Fig. 9. This arrangement has the great advantage that the light is gathered by two small or medium-sized telescopes and then combined by the Kösters prism. As a result, much fainter magnitudes can be reached than have ever before been possible. Beavers estimates his limiting magnitude with the 1" x 6" mirrors to be about 2nd magnitude. The intensity interferometer as described by R. Q. Twiss in Space Physics and Radio Astronomy has been designed to measure stellar diameters of stars brighter than magnitude 3.5 provided that such a star is hot enough not to be appreciably resolved by an individual mirror. The design which we propose could go beyond this limit using only two 12-inch aperture instruments. The use of photoelectric detection and recording techniques should enable us to work on the same part of the visibility curve as Beavers, and permit us to measure quite accurately the effects of scintillation on coherence loss.

We plan to submit a proposal for funds to construct and do research with an instrument such as this. Details on the design of this stellar interferometer will be included in the proposal. One important advantage of the increased amount of light available with the instrument would be the ability to use narrow-band optical filters which would define the wavelength of the measurement as well as reduce the seeing effects. Twiss(1964) points out that if a re-engineered version of the Michelson stellar interferometer is to be built, it should be able to measure accurately the amplitude of the visibility curve at any point within the range of the interferometer base line. Such an instrument would be of considerable value to astronomy if its operation were not confined to nights of exceptional seeing. We believe the Kösters instrument will meet both of these specifications.

APPENDIX A Table of Filters

Filter	Peak (Å)	Halfwidth (Å)	Type
A	4200	90	Interference 2nd Order
B	5500	200	Interference 1st Order
C	5920	140	Interference 2nd Order
D	Cut off at 4950		Absorption

APPENDIX B Results of the interferometer tests on the Leander McCormick 32-inch reflector.

Plot Table	Interferogram	Date	Time (EST)	Source	Filter	Exp. Time (Sec.)
1	AB - 6	5/26/65	22:30	Arcturus	B	16
	AB - 7	"	22:33	"	B	24
	AB - 12	"	23:05	"	B	16
2	AB - 2	"	22:20	"	B	20
	X - 2	"	23:20	"	B	12
	AB - 9	"	22:48	"	B	12
3	SN	8/12/65	22:00	Vega	D	4
4	WE	"	22:10	"	D	4
5	SW - NE	"	22:20	"	D	3
6	SE - NW	"	22:26	"	D	.5

The following plots represent the deviations of the wave front of the Mc Cormick 32-inch reflector from a spherical wave front. The deviations, δ_{λ}, are expressed in wavelengths determined by the filters as listed in the preceding table, D represents inches along the diameter. The direction of shear is indicated below the plot and the size of the arrows indicate the probable error for each point.

FAN MOUNTAIN 32-INCH REFLECTOR - PRIOR TO AUG 65

DIRECTION OF SHEAR: SN

REFERENCE POINT	INTERFEROGRAM IDENTIFICATION AB-6	AB-7	AB-12	NORMAL POINTS
0	-0.310	-0.370	-0.417	-0.366
1	-0.187	-0.192	-0.262	-0.214
2	0.116	0.115	0.029	0.087
3	0.242	0.277	0.220	0.246
4	0.327	0.333	0.331	0.330
5	0.262	0.275	0.300	0.279
6	0.059	0.078	0.135	0.091
7	-0.213	-0.186	-0.201	-0.200
8	-0.350	-0.508	-0.342	-0.400
16	-0.012	0.029	0.009	0.009
17	-0.083	-0.061	-0.051	-0.065
18	-0.095	-0.078	-0.032	-0.068
19	-0.022	-0.043	-0.021	-0.029
20	0.031	-0.010	-0.025	-0.001
21	0.086	0.042	0.003	0.044
22	0.129	0.069	0.032	0.077
23	0.068	0.047	0.042	0.052
24	-0.103	0.003	0.042	-0.019

PROBABLE ERROR FOR ANY MEASUREMENT: 0.023

TABLE 1

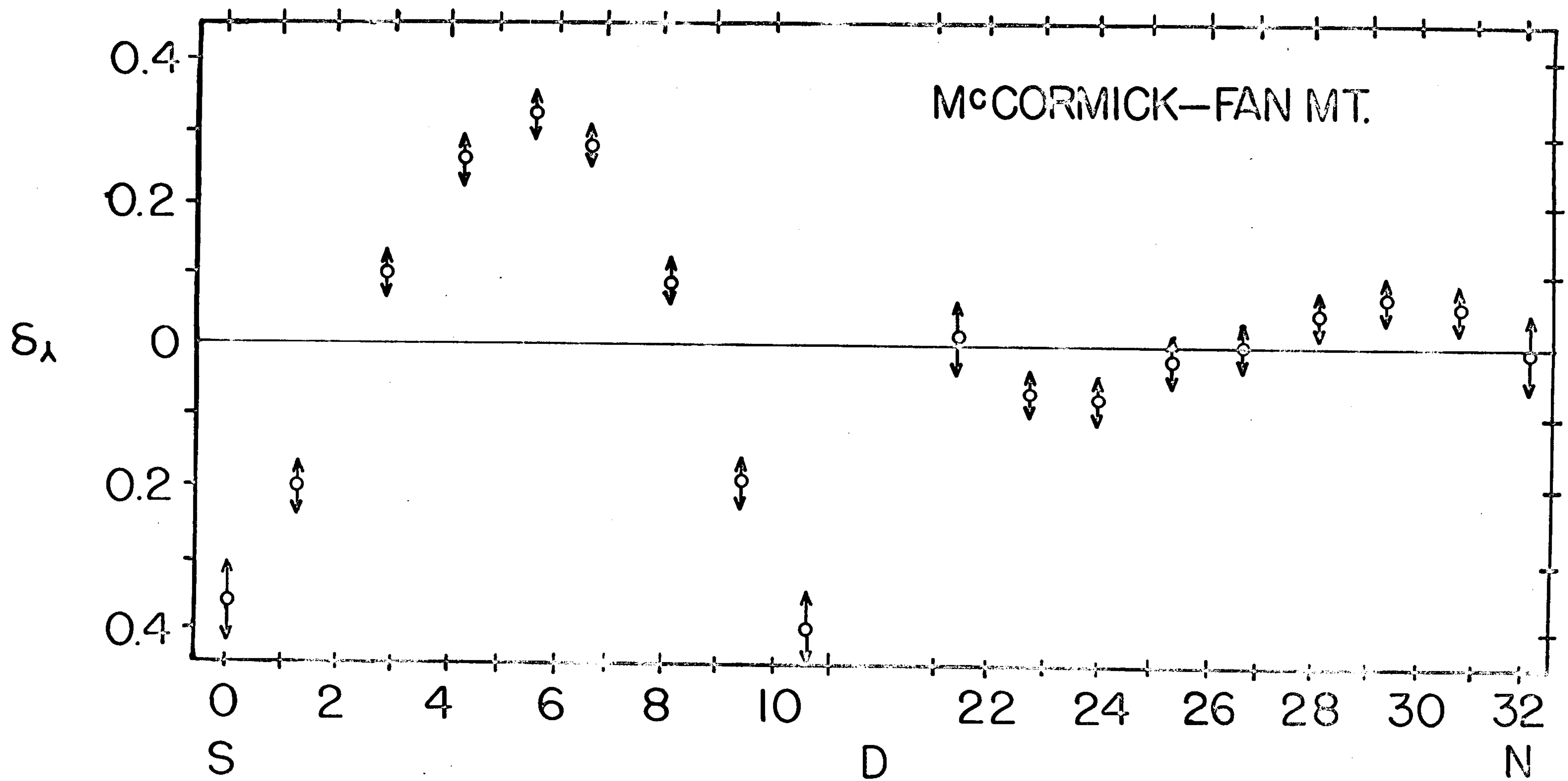

Plot 1

FAN MOUNTAIN 32-INCH REFLECTOR - PRIOR TO AUG 65

DIRECTION OF SHEAR: WE

REFERENCE POINT	INTERFEROGRAM IDENTIFICATION AB-2	X-2	AB-9	NORMAL POINTS
0	-0.413	-0.226	-0.153	-0.264
1	-0.064	-0.033	-0.008	-0.035
2	0.172	0.098	0.077	0.116
3	0.294	0.166	0.105	0.188
4	0.311	0.172	0.103	0.195
5	0.223	0.115	0.068	0.135
6	-0.006	0.025	0.014	0.011
7	-0.188	-0.089	-0.055	-0.111
8	-0.330	-0.227	-0.150	-0.236
16	-0.102	-0.102	-0.143	-0.116
17	-0.033	-0.071	-0.053	-0.052
18	0.012	-0.022	0.024	0.005
19	0.038	0.034	0.065	0.046
20	0.037	0.098	0.092	0.076
21	0.038	0.117	0.095	0.083
22	0.031	0.085	0.059	0.058
23	-0.004	0.003	-0.017	-0.006
24	-0.017	-0.141	-0.122	-0.093

PROBABLE ERROR FOR ANY MEASUREMENT: 0.035

TABLE 2

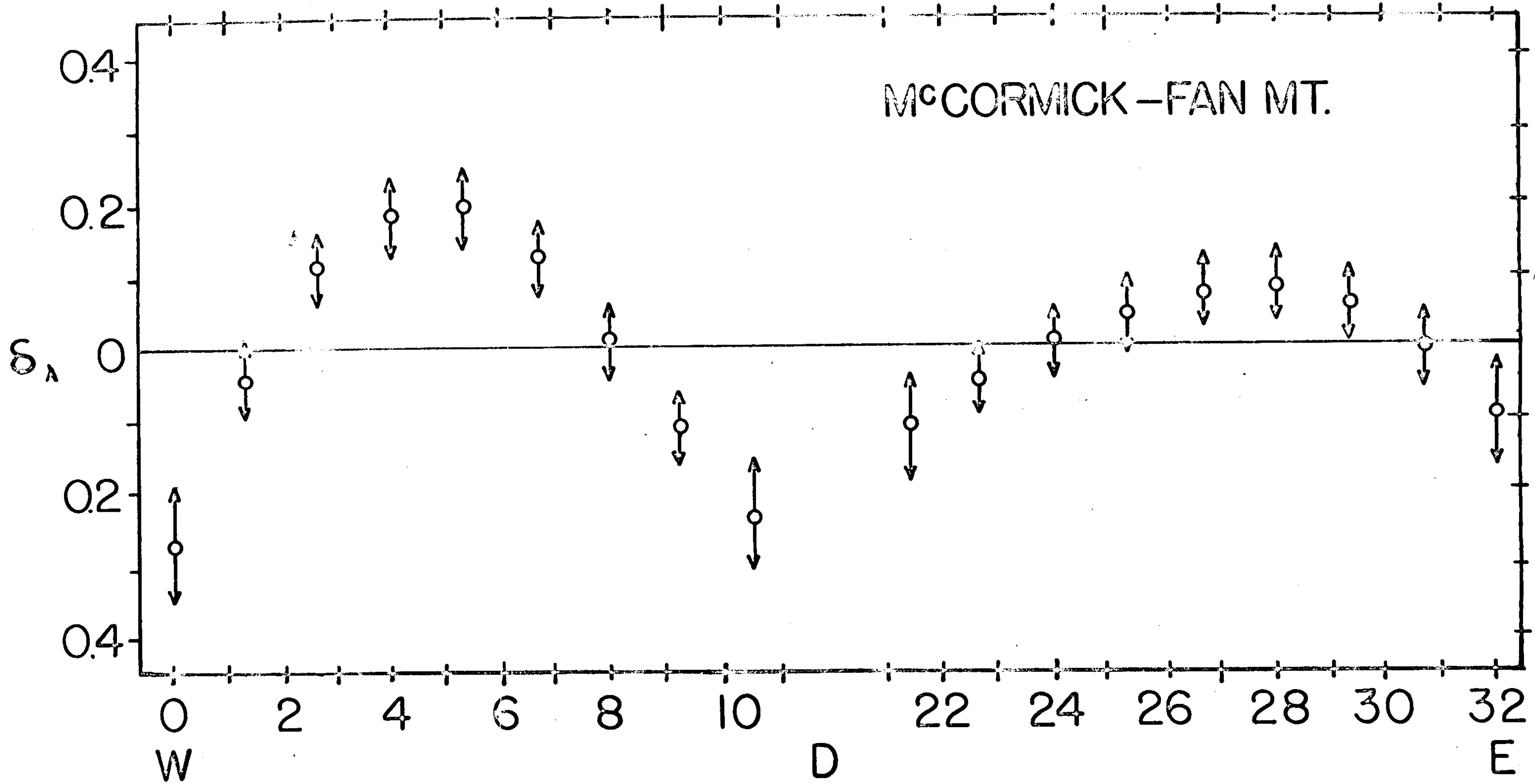
McCORMICK – FAN MT.
0.4
0.2
δ_λ 0
0.2
0.4
0
2
4
6
8
10
22
24
26
28
30
32
W
D
E

Plot 2

FAN MOUNTAIN 32-INCH REFLECTOR - AFTER AUG 65

DIRECTION OF SHEAR: 4 DIRECTIONS

INTERFEROGRAM IDENTIFICATION

REFERENCE POINT	SN	WE	SW-NE	SE-NW
0	-0.649	-0.999	0.016	-0.082
1	-0.154	0.192	0.175	0.053
2	0.207	0.346	0.156	0.145
3	0.368	0.374	0.073	0.161
4	0.375	0.339	-0.046	0.002
5	0.274	0.206	-0.176	-0.100
6	0.145	0.110	-0.215	-0.106
7	0.047	0.047	-0.190	-0.055
8	-0.077	-0.023	-0.129	-0.035
9	-0.220	-0.092	0.022	-0.006
10	-0.317	-0.171	0.315	0.022
11	******	-0.302	******	******
21	0.363	******	-0.361	-0.298
22	0.066	0.134	-0.251	-0.192
23	-0.092	0.046	-0.045	-0.104
24	-0.199	0.001	-0.030	-0.034
25	-0.236	-0.162	0.048	0.061
26	-0.228	-0.225	0.160	0.146
27	-0.152	-0.177	0.372	0.248
28	-0.014	0.031	0.415	0.328
29	0.115	0.158	0.378	0.345
30	0.313	0.143	0.277	0.294
31	0.342	0.078	-0.055	0.134
32	-0.269	-0.027	-0.908	-0.929

TABLE 3,4,5,6

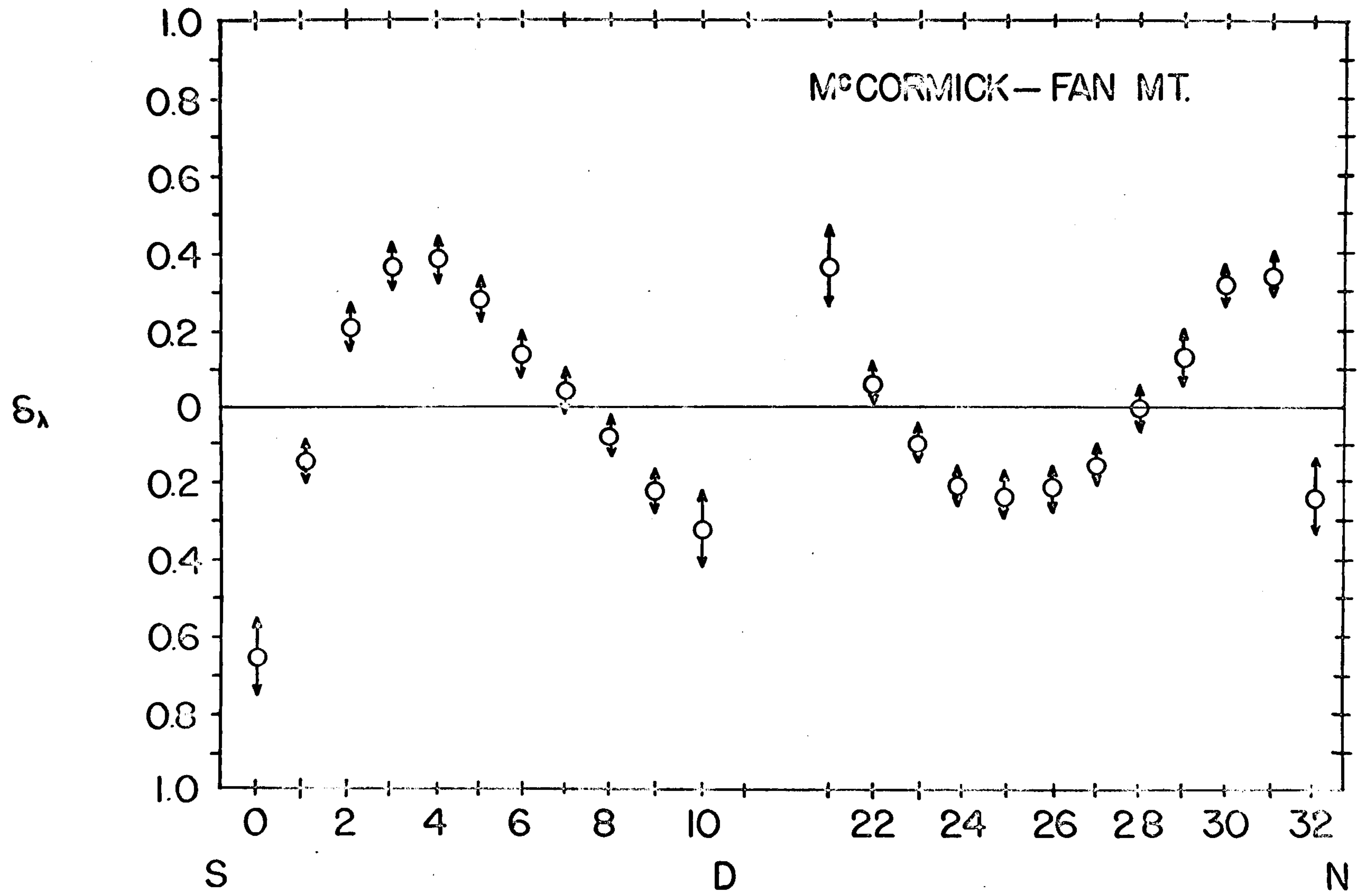
McCORMICK — FAN MT.
1.0
0.8
0.6
0.4
0.2
0
0.2
0.4
0.6
0.8
1.0
δ_λ
0
2
4
6
8
10
22
24
26
28
30
32
S
D
N

Plot 3

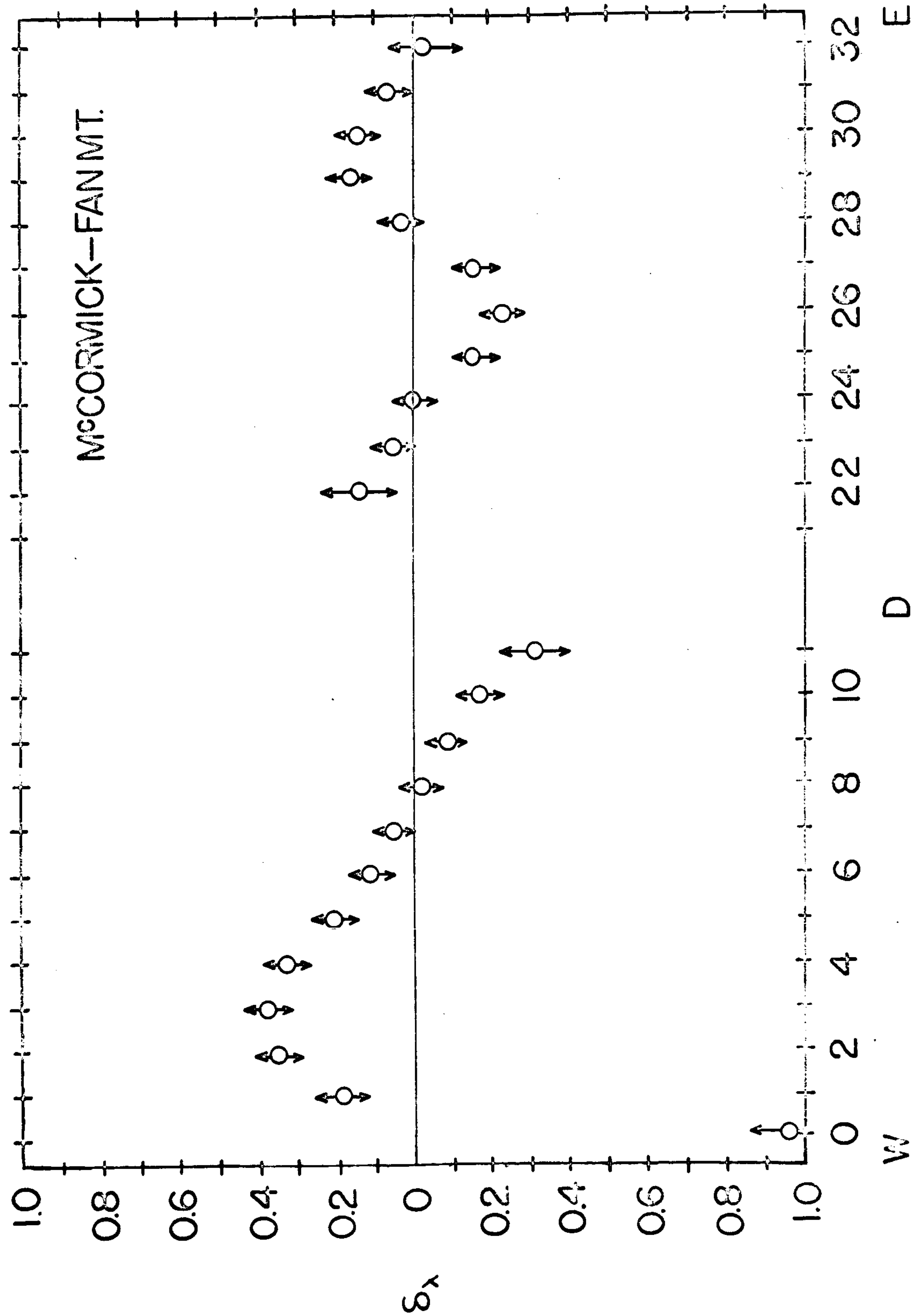
McCORMICK—FAN MT.
1.0
0.8
0.6
0.4
0.2
0
0.2
0.4
0.6
0.8
1.0
W
0
2
4
6
8
10
D
22
24
26
28
30
32
E

Plot x

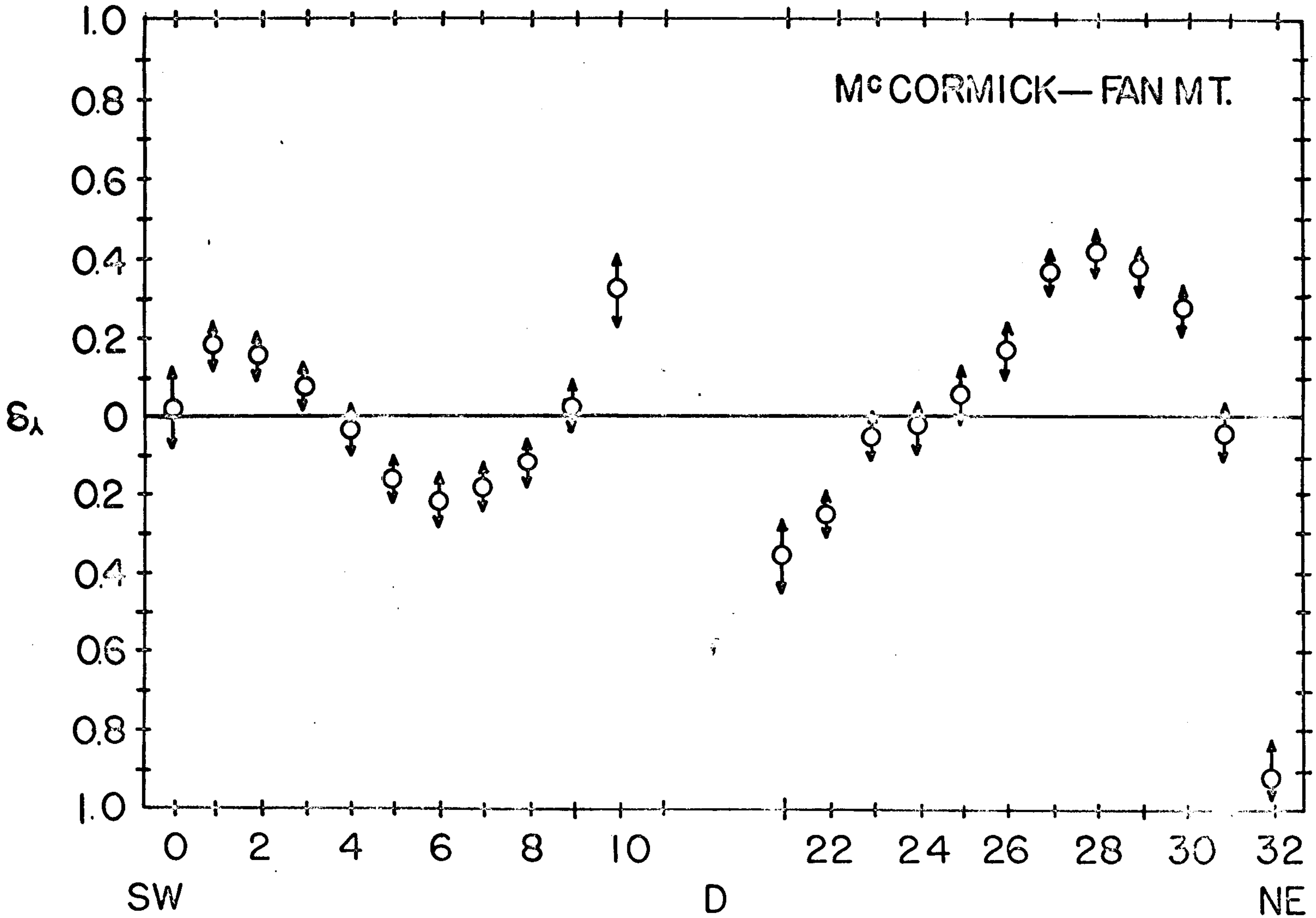

McCORMICK—FAN MT.
1.0
0.8
0.6
0.4
0.2
0
0.2
0.4
0.6
0.8
1.0
δλ
0
2
4
6
8
10
22
24
26
28
30
32
SW
D
NE

Plot 5

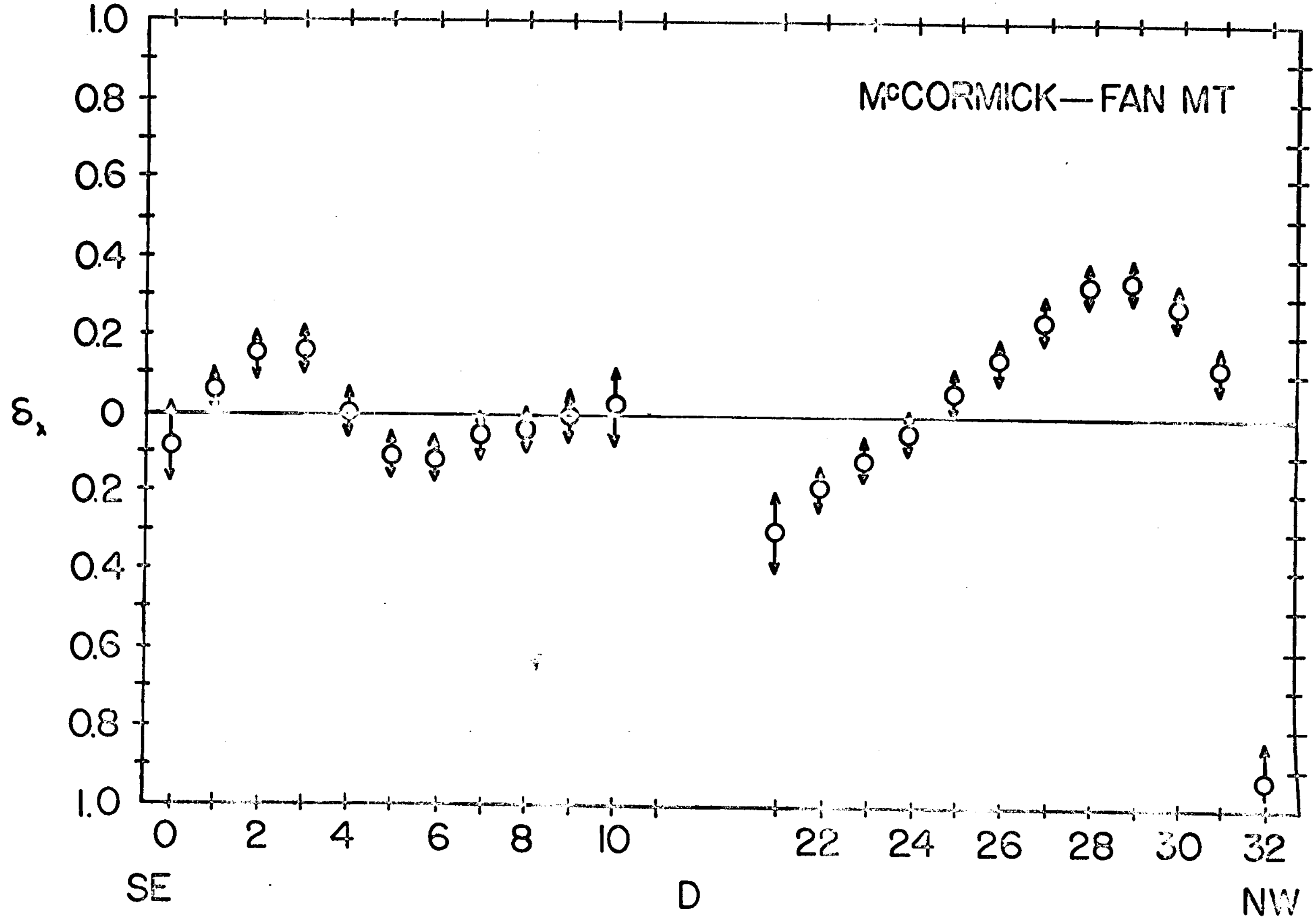

McCORMICK—FAN MT
1.0
0.8
0.6
0.4
0.2
0
0.2
0.4
0.6
0.8
1.0
δ_x
0
2
4
6
8
10
22
24
26
28
30
32
SE
D
NW

Plot 6

APPENDIX C: Results of the interferometer tests on the Mt. Cuba 24-inch reflector.

Plot Table	Interferogram	Date	Time (EST)	Source	Filter	Exp. Time (sec.)
7	1-1	8/5/65	22:30	Vega	B	15
	1-2	"	22:31	"	"	20
	1-3	"	22:32	"	"	15
	1-4	"	22:33	"	"	10
	2-3	"	23:04	"	"	20
	2-4	"	23:06	"	"	15
	2-5	"	23:07	"	"	10
8	1-5	"	22:37	"	"	10
	1-6	"	22:38	"	"	15
	1-7	"	22:39	"	"	20
	1-8	"	22:40	"	"	15
	2-6	"	23:15	"	"	10
	2-7	"	23:17	"	"	15

The following plots represent the deviations of the wave front of the Mt. Cuba 24-inch reflector from a spherical wave front. The deviations, δ, are expressed in wavelengths determined by the filters as listed in the preceding table; D represents inches along the diameter. The direction of shear is indicated below the plot and the size of the arrows indicate the probable error for each point.

MT. CUBA 24-INCH REFLECTOR

DIRECTION OF SHEAR: SN

INTERFEROGRAM IDENTIFIC

REFERENCE POINT	1-1	1-2	1-3	1-4
0	0.043	-0.010	0.046	0.027
1	0.029	-0.059	-0.027	-0.070
2	-0.011	-0.070	-0.056	-0.070
3	-0.049	-0.043	-0.066	-0.001
4	-0.103	0.002	-0.067	0.037
5	-0.105	0.055	-0.043	0.042
6	-0.033	0.076	0.022	0.026
7	0.061	0.055	0.098	0.003
8	0.168	-0.008	0.097	-0.001
16	0.370	0.430	0.440	0.290
17	0.137	0.135	0.253	0.146
18	-0.024	-0.031	0.028	-0.028
19	-0.171	-0.268	-0.166	-0.166
20	-0.315	-0.408	-0.318	-0.243
21	-0.307	-0.391	-0.388	-0.253
22	-0.155	-0.129	-0.173	-0.155
23	0.069	0.153	0.132	0.052
24	0.397	0.593	0.548	0.357

PROBABLE ERROR FOR ANY ME

1

TABLE 7

.TIUN

2-3	2-4	2-5	NORMAL POINTS
0.125	-0.018	0.007	0.031
-0.054	-0.049	-0.051	-0.040
-0.117	-0.043	-0.056	-0.061
-0.116	-0.013	-0.027	-0.045
-0.049	0.032	0.025	-0.018
0.014	0.053	0.071	0.012
0.081	0.049	0.070	0.042
0.114	-0.010	0.022	0.050
******	******	-0.062	0.036
0.374	0.436	0.373	0.388
0.195	0.133	0.139	0.163
-0.029	-0.094	-0.112	-0.041
-0.228	-0.236	-0.269	-0.215
-0.371	-0.293	-0.323	-0.324
-0.289	-0.275	-0.273	-0.311
-0.122	-0.161	-0.135	-0.147
0.081	0.078	0.160	0.104
0.389	0.411	0.466	0.452

SUREMENT: 0.032

2

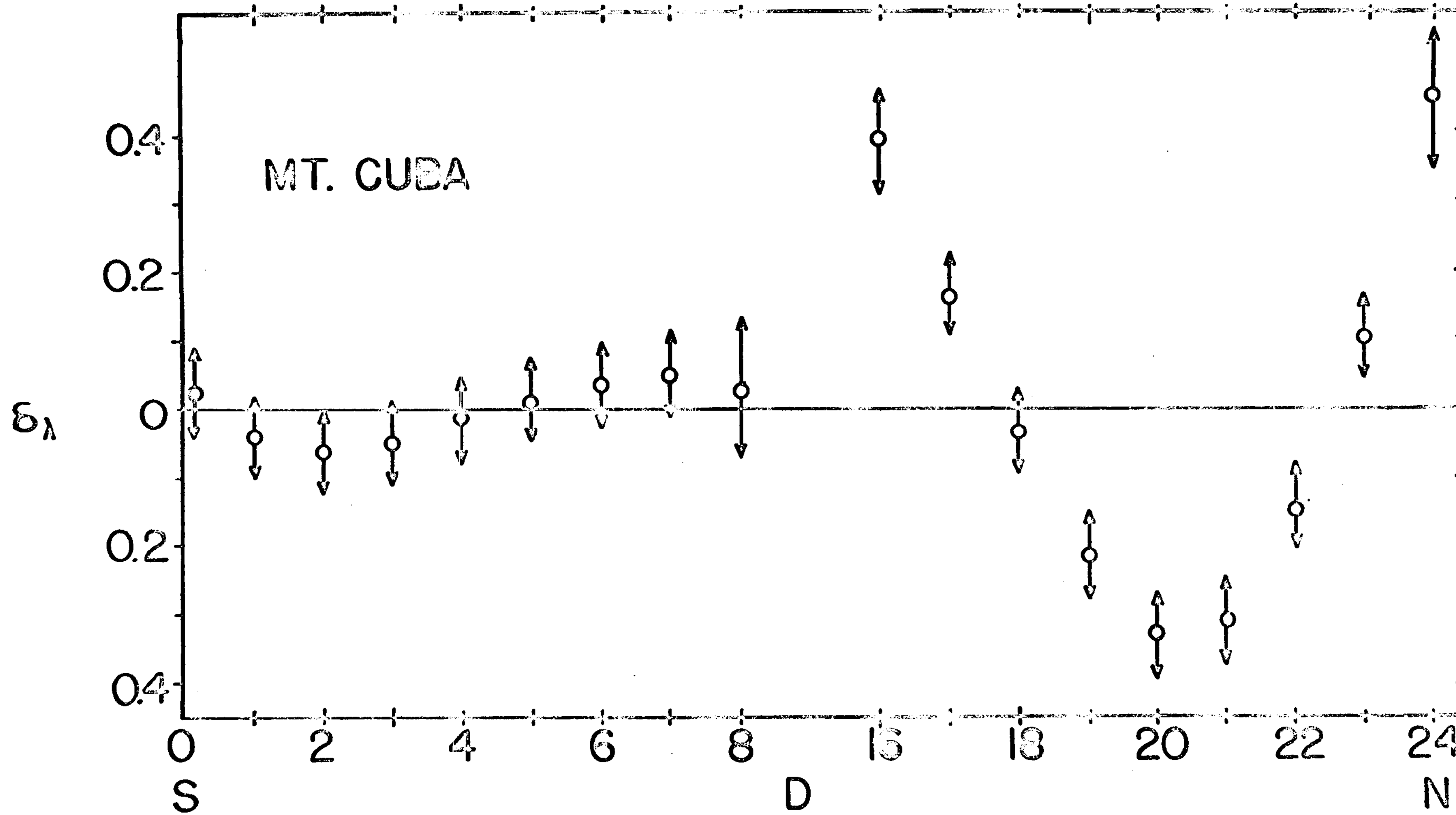

Plot 7

MT. CUBA 24-INCH REFLECTOR

DIRECTION OF SHEAR: WE

REFERENCE POINT	1-5	1-6	1-7	1-8
			INTERFEROGRAM	IDENTI
0	-0.310	-0.345	-0.268	-0.270
1	-0.076	-0.067	-0.084	-0.072
2	0.077	0.123	0.059	0.071
3	0.156	0.235	0.142	0.160
4	0.198	0.250	0.174	0.194
5	0.186	0.156	0.175	0.164
6	0.104	0.063	0.135	0.079
7	-0.061	-0.170	-0.025	-0.061
8	-0.276	-0.316	-0.307	-0.265
16	0.528	0.425	0.409	0.324
17	0.172	0.163	0.182	0.093
18	-0.135	-0.068	-0.057	-0.063
19	-0.324	-0.246	-0.246	-0.173
20	-0.394	-0.362	-0.365	-0.258
21	-0.336	-0.326	-0.346	-0.257
22	-0.149	-0.169	-0.137	-0.112
23	0.147	0.101	0.101	0.100
24	0.491	0.482	0.508	0.346

PROBABLE ERROR FOR ANY

TABLE 8

1

ICATION

2-6	2-7	NORMAL POINTS
-0.158	-0.193	-0.257
-0.077	-0.075	-0.075
0.001	0.020	0.059
0.077	0.082	0.142
0.149	0.121	0.181
0.148	0.138	0.161
0.084	0.102	0.095
-0.042	-0.007	-0.061
-0.182	-0.188	-0.256
0.387	0.581	0.442
0.154	0.188	0.159
-0.093	-0.107	-0.087
-0.242	-0.325	-0.259
-0.305	-0.436	-0.353
-0.260	-0.399	-0.321
-0.128	-0.215	-0.160
0.090	0.117	0.109
0.396	0.595	0.470

EASUREMENT: 0.033

2

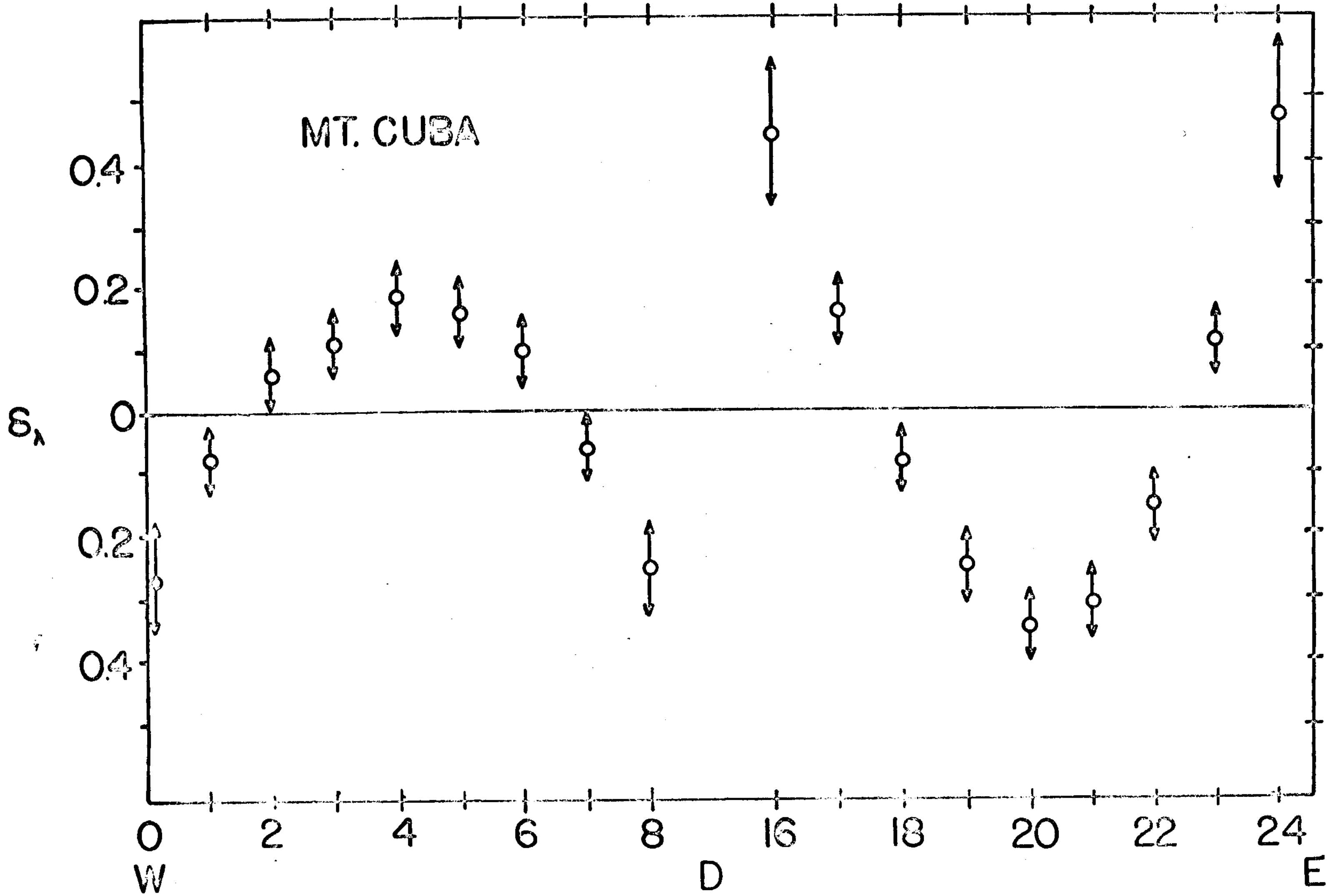

Plot 8

APPENDIX D: Results of the interferometer tests on the Kitt Peak 84-inch reflector.

Plot Table	Interferogram	Date	Time (MST)	Source	Filter	Exp. Time (sec.)
9	4-1	9/9/65	8:31	Vega	D	3
	4-10	"	8:40	"	D	1
	6-1	9/10/65	8:16	"	B	5
	6-5	"	8:20	"	B	5
10	4-3	9/9/65	8:33	"	D	3
	4-11	"	8:41	"	D	3
	6-2	9/10/65	8:17	"	B	5
	6-6	"	8:21	"	B	5
11	4-8	9/9/65	8:38	"	D	1
	4-15	"	8:45	"	D	3
	6-4	9/10/65	8:19	"	B	5
	6-8	"	8:23	"	B	5
12	4-6	9/9/65	8:36	"	D	1
	4-13	"	8:43	"	D	3
	6-3	9/10/65	8:18	"	B	5
	6-7	"	8:22	"	B	5

The following plots represent the deviations of the wave front of the Kitt Peak 84-inch reflector from a spherical wave front. The deviations, δ_λ, are expressed in wavelengths determined by the filters as listed in the preceding table; D represents inches along the diameter. The direction of shear is indicated as the angle made with the north-south line of the mirror. The size of the arrow in the upper left hand corner indicates the size of the probable error for all the points.

KITT PEAK 84-INCH REFLECTOR

DIRECTION OF SHEAR: 30(210)

REFERENCE POINT	INTERFEROGRAM IDENTIFICATION 4-1	4-10	6-1	6-5	NORMAL POINTS
0	******	******	******	******	******
1	-0.069	-0.567	-0.213	-0.212	-0.265
2	-0.056	-0.389	-0.129	-0.465	-0.260
3	-0.056	-0.190	-0.112	-0.274	-0.158
4	0.020	0.050	0.020	-0.121	-0.008
5	0.064	0.146	0.103	0.046	0.090
6	0.050	0.298	0.120	0.135	0.151
7	0.064	0.330	0.191	0.187	0.193
8	0.138	0.333	0.181	0.202	0.214
9	0.073	0.306	0.139	0.180	0.175
10	0.001	0.197	0.083	0.181	0.116
11	0.019	0.148	0.000	0.235	0.101
12	0.049	0.159	-0.024	0.282	0.117
13	0.082	0.158	0.035	0.262	0.134
14	0.018	0.110	0.038	0.185	0.088
15	-0.036	0.016	-0.007	0.050	-0.007
16	-0.079	-0.090	-0.079	-0.131	-0.095
17	-0.105	-0.184	-0.154	-0.350	-0.198
18	-0.127	-0.321	-0.192	-0.605	-0.311
19	******	******	******	******	******
49	******	******	******	******	******
50	-0.633	-0.362	-0.327	0.114	-0.302
51	-0.465	-0.190	-0.160	0.035	-0.195
52	-0.237	-0.061	-0.112	-0.041	-0.113
53	-0.065	-0.030	-0.030	-0.094	-0.055
54	0.051	-0.055	0.007	-0.084	-0.020
55	0.193	0.000	0.012	-0.061	0.036
56	0.220	0.067	0.022	-0.075	0.059
57	0.250	0.064	0.019	-0.097	0.059
58	0.240	0.023	0.084	-0.135	0.053
59	0.291	0.127	0.135	-0.061	0.123
60	0.402	0.221	0.230	0.047	0.225
61	0.373	0.266	0.210	0.097	0.236
62	0.287	0.241	0.218	0.170	0.229
63	0.264	0.228	0.265	0.196	0.238
64	0.173	0.215	0.264	0.195	0.212
65	-0.039	0.061	0.116	0.138	0.069
66	-0.266	-0.082	-0.118	0.022	-0.111
67	-0.433	-0.296	-0.350	-0.130	-0.302
68	-0.607	-0.437	-0.480	-0.239	-0.441
69	******	******	******	******	******

PROBABLE ERROR FOR ANY MEASUREMENT: 0.074

TABLE 9

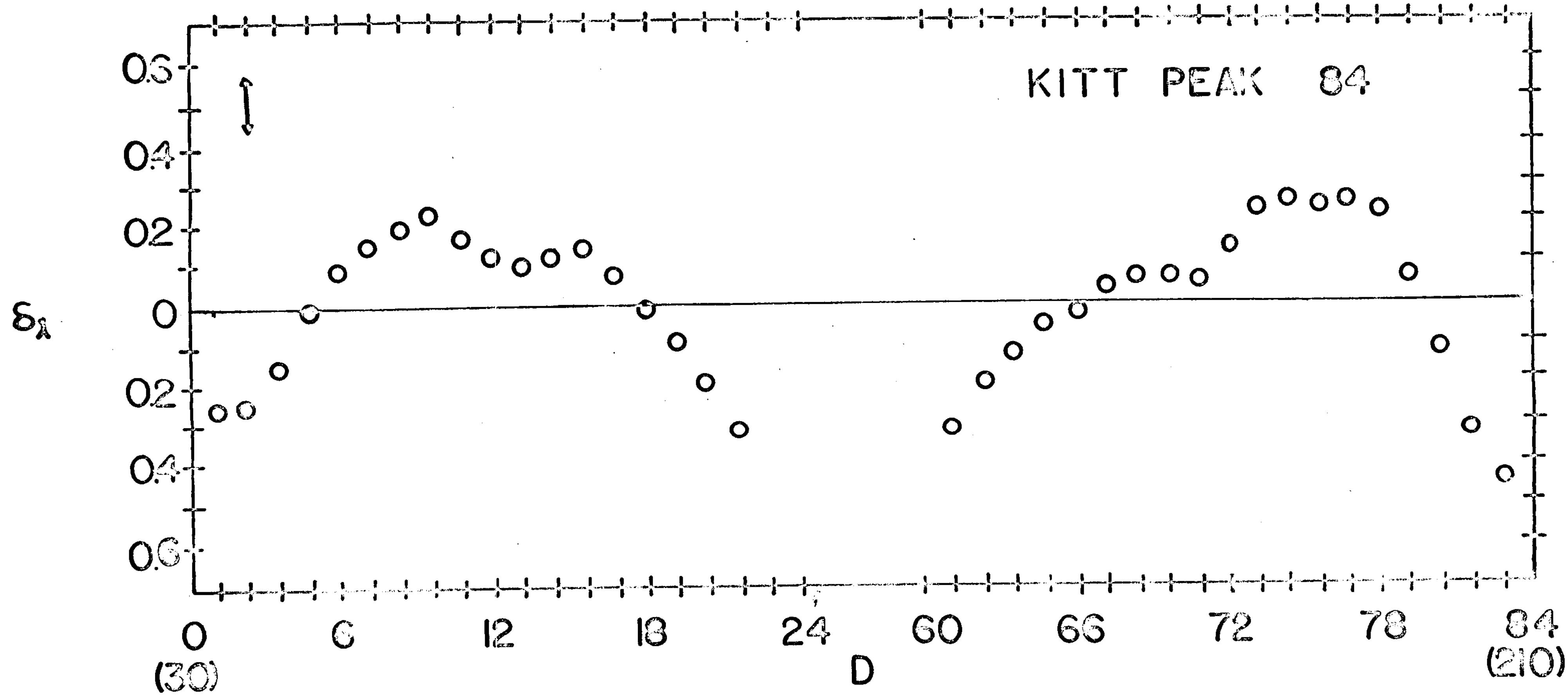
KITT PEAK 84
0.6
0.4
0.2
0
0.2
0.4
0.6
δ_λ
0
(30)
6
12
18
24
60
66
72
78
84
(210)
D

Plot 9

KITT PEAK 84-INCH REFLECTOR

DIRECTION OF SHEAR: 345(165)

REFERENCE POINT	INTERFEROGRAM IDENTIFICATION 4-3	4-11	6-2	6-6	NORMAL POINTS
0	******	******	******	******	******
1	-0.516	-0.846	-0.398	-0.914	-0.668
2	-0.384	-0.524	-0.263	-0.496	-0.417
3	-0.173	-0.211	-0.043	-0.099	-0.131
4	0.051	0.031	0.074	0.128	0.071
5	0.140	0.250	0.205	0.310	0.226
6	0.243	0.404	0.273	0.362	0.321
7	0.270	0.458	0.192	0.387	0.327
8	0.282	0.412	0.223	0.434	0.338
9	0.291	0.355	0.172	0.408	0.306
10	0.238	0.313	0.094	0.331	0.244
11	0.207	0.303	-0.055	0.276	0.183
12	0.156	0.291	-0.031	0.242	0.165
13	0.152	0.221	-0.006	0.113	0.120
14	0.106	0.079	-0.010	-0.044	0.033
15	-0.005	-0.051	-0.083	-0.180	-0.080
16	-0.177	-0.211	-0.089	-0.295	-0.193
17	-0.244	-0.293	-0.096	-0.429	-0.266
18	-0.307	-0.388	-0.078	-0.534	-0.327
19	-0.331	-0.592	-0.131	-0.534	-0.397
20	******	******	******	******	******
50	******	******	******	******	******
51	-0.129	-0.350	-0.395	-0.216	-0.272
52	-0.059	-0.159	-0.221	-0.165	-0.151
53	-0.043	-0.024	-0.059	-0.109	-0.059
54	-0.012	0.057	0.021	-0.115	-0.012
55	-0.002	0.050	0.086	-0.036	0.025
56	-0.046	0.054	0.151	0.050	0.052
57	0.008	0.070	0.143	0.061	0.071
58	-0.006	-0.069	0.077	0.070	0.018
59	-0.043	-0.077	0.058	0.006	-0.015
60	-0.004	0.030	0.127	0.045	0.050
61	0.137	0.176	0.181	0.190	0.171
62	0.174	0.217	0.135	0.211	0.184
63	0.144	0.203	0.108	0.221	0.169
64	0.142	0.134	0.114	0.118	0.127
65	0.070	0.077	-0.027	0.037	0.039
66	-0.006	0.031	-0.051	0.026	0.000
67	-0.084	-0.003	-0.175	-0.178	-0.110
68	-0.233	-0.119	-0.273	-0.408	-0.259
69	******	******	******	******	******

PROBABLE ERROR FOR ANY MEASUREMENT: 0.060

TABLE 10

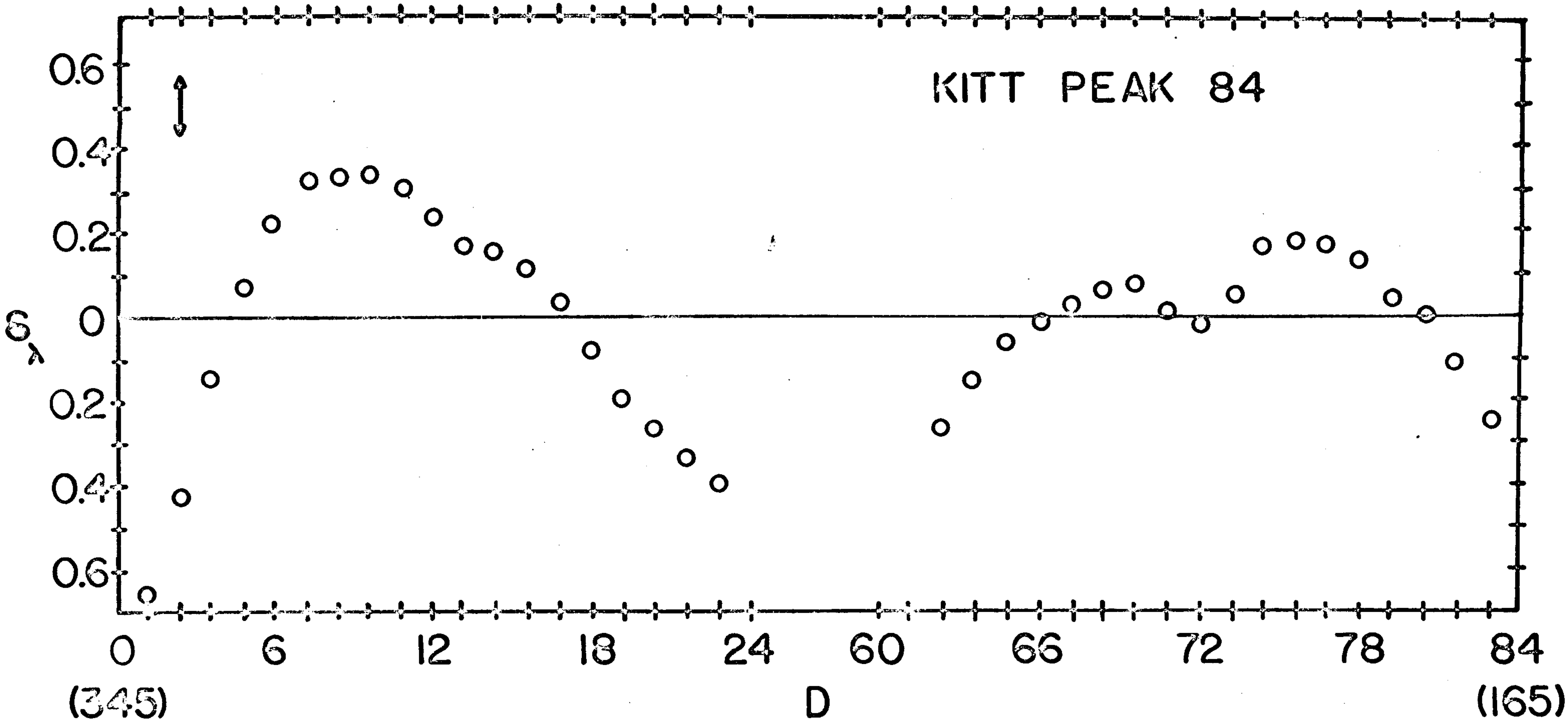
KITT PEAK 84
0.6
0.4
0.2
0
0.2
0.4
0.6
δ_λ
0
6
12
18
24
60
66
72
78
84
(345)
D
(165)

Plot 10

KITT PEAK 84-INCH REFLECTOR

DIRECTION OF SHEAR: 255(75)

REFERENCE POINT	INTERFEROGRAM IDENTIFICATION 4-8	4-15	6-4	6-8	NORMAL POINTS
0	******	******	******	******	******
1	-0.222	-0.463	-0.270	-0.429	-0.346
2	-0.123	-0.265	-0.194	-0.291	-0.218
3	-0.024	-0.141	-0.081	-0.142	-0.097
4	0.036	-0.033	0.001	0.018	0.006
5	0.017	0.077	0.101	0.123	0.080
6	0.008	0.189	0.206	0.181	0.146
7	0.040	0.232	0.186	0.293	0.188
8	0.083	0.278	0.177	0.291	0.207
9	0.137	0.290	0.169	0.258	0.214
10	0.171	0.197	0.083	0.161	0.153
11	0.157	0.130	0.021	0.151	0.115
12	0.153	0.089	0.003	0.128	0.093
13	0.099	0.074	0.053	0.140	0.092
14	0.057	0.086	0.073	0.068	0.071
15	-0.005	0.076	0.061	-0.064	0.017
16	-0.056	0.028	0.003	-0.142	-0.042
17	-0.107	-0.049	-0.114	-0.167	-0.109
18	-0.186	-0.123	-0.220	-0.222	-0.188
19	-0.235	-0.267	-0.257	-0.355	-0.278
20	******	******	******	******	******
49	******	******	******	******	******
50	-0.371	-0.097	-0.619	-0.444	-0.383
51	-0.275	-0.093	-0.436	-0.280	-0.271
52	-0.139	-0.105	-0.218	-0.165	-0.157
53	-0.032	-0.083	-0.047	-0.019	-0.045
54	0.036	0.000	0.118	0.086	0.060
55	0.165	0.025	0.226	0.077	0.123
56	0.224	0.026	0.240	-0.046	0.111
57	0.214	-0.013	0.243	-0.032	0.103
58	0.175	0.007	0.341	0.119	0.161
59	0.157	0.053	0.406	0.323	0.235
60	0.169	0.125	0.359	0.434	0.272
61	0.162	0.140	0.313	0.443	0.265
62	0.116	0.182	0.219	0.389	0.227
63	0.061	0.166	0.078	0.221	0.131
64	-0.054	0.093	-0.136	-0.010	-0.027
65	-0.208	-0.038	-0.425	-0.190	-0.215
66	-0.401	-0.143	-0.660	-0.348	-0.388
67	******	******	******	******	******
68	******	******	******	******	******

PROBABLE ERROR FOR ANY MEASUREMENT: 0.061

TABLE 11

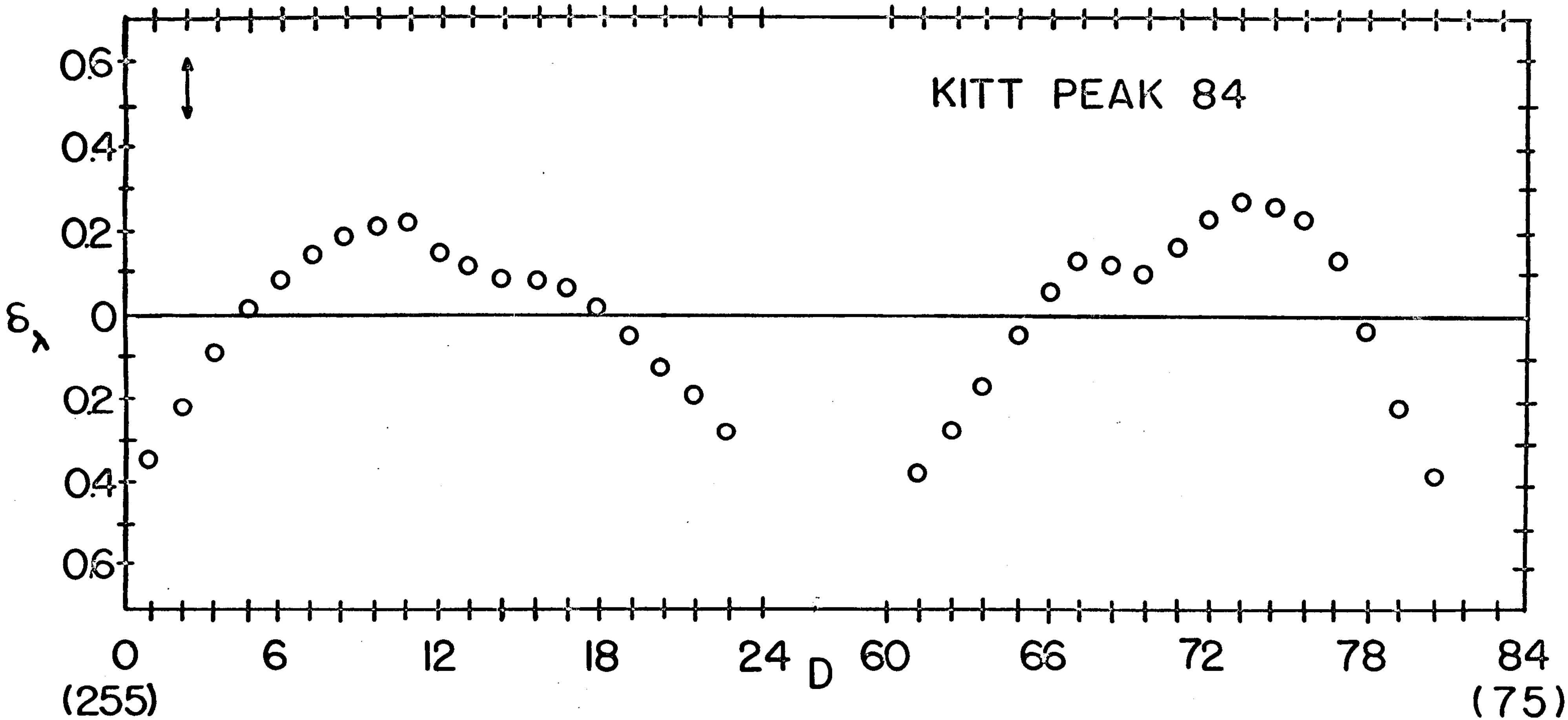
KITT PEAK 84
0.6
0.4
0.2
0
0.2
0.4
0.6
δ_λ
0
(255)
6
12
18
24
D
60
66
72
78
84
(75)

Plot 11

KITT PEAK 84-INCH REFLECTOR

DIRECTION OF SHEAR: 300(120)

REFERENCE POINT	INTERFEROGRAM IDENTIFICATION 4-6	4-13	6-3	6-[illegible]	NORMAL POINTS
0	******	******	******	******	******
1	-0.399	-0.505	-0.376	-0.442	-0.430
2	-0.292	-0.418	-0.313	-0.344	-0.342
3	-0.156	-0.189	-0.214	-0.200	-0.190
4	0.007	-0.005	-0.061	-0.012	-0.018
5	0.128	0.114	0.064	0.137	0.111
6	0.182	0.169	0.176	0.247	0.193
7	0.266	0.219	0.329	0.318	0.283
8	0.294	0.235	0.416	0.349	0.323
9	0.268	0.196	0.379	0.341	0.296
10	0.198	0.102	0.263	0.224	0.197
11	0.147	0.024	0.203	0.155	0.132
12	0.123	0.001	0.149	0.113	0.097
13	0.044	-0.017	0.054	0.032	0.028
14	-0.005	-0.039	-0.083	-0.005	-0.033
15	-0.051	-0.106	-0.127	-0.080	-0.091
16	-0.092	-0.147	-0.180	-0.194	-0.153
17	-0.140	-0.094	-0.274	-0.265	-0.193
18	-0.241	-0.044	-0.405	-0.374	-0.266
19	******	******	******	******	******
51	******	******	******	******	******
52	-0.537	0.017	-0.566	-0.167	-0.313
53	-0.358	-0.006	-0.339	-0.145	-0.212
54	-0.151	-0.032	-0.175	-0.079	-0.109
55	0.002	-0.064	-0.052	-0.052	-0.041
56	0.100	-0.119	0.113	-0.064	0.008
57	0.199	-0.120	0.153	-0.032	0.050
58	0.271	-0.035	0.179	0.044	0.115
59	0.372	0.015	0.327	0.165	0.220
60	0.335	0.120	0.409	0.197	0.265
61	0.242	0.171	0.387	0.206	0.252
62	0.143	0.168	0.303	0.193	0.202
63	0.049	0.039	0.195	0.157	0.110
64	-0.040	-0.034	0.062	0.062	0.012
65	-0.054	-0.061	-0.096	-0.051	-0.065
66	-0.086	-0.103	-0.346	-0.204	-0.185
67	-0.173	-0.319	-0.554	-0.230	-0.319
68	******	******	******	******	******

PROBABLE ERROR FOR ANY MEASUREMENT: 0.060

TABLE 12

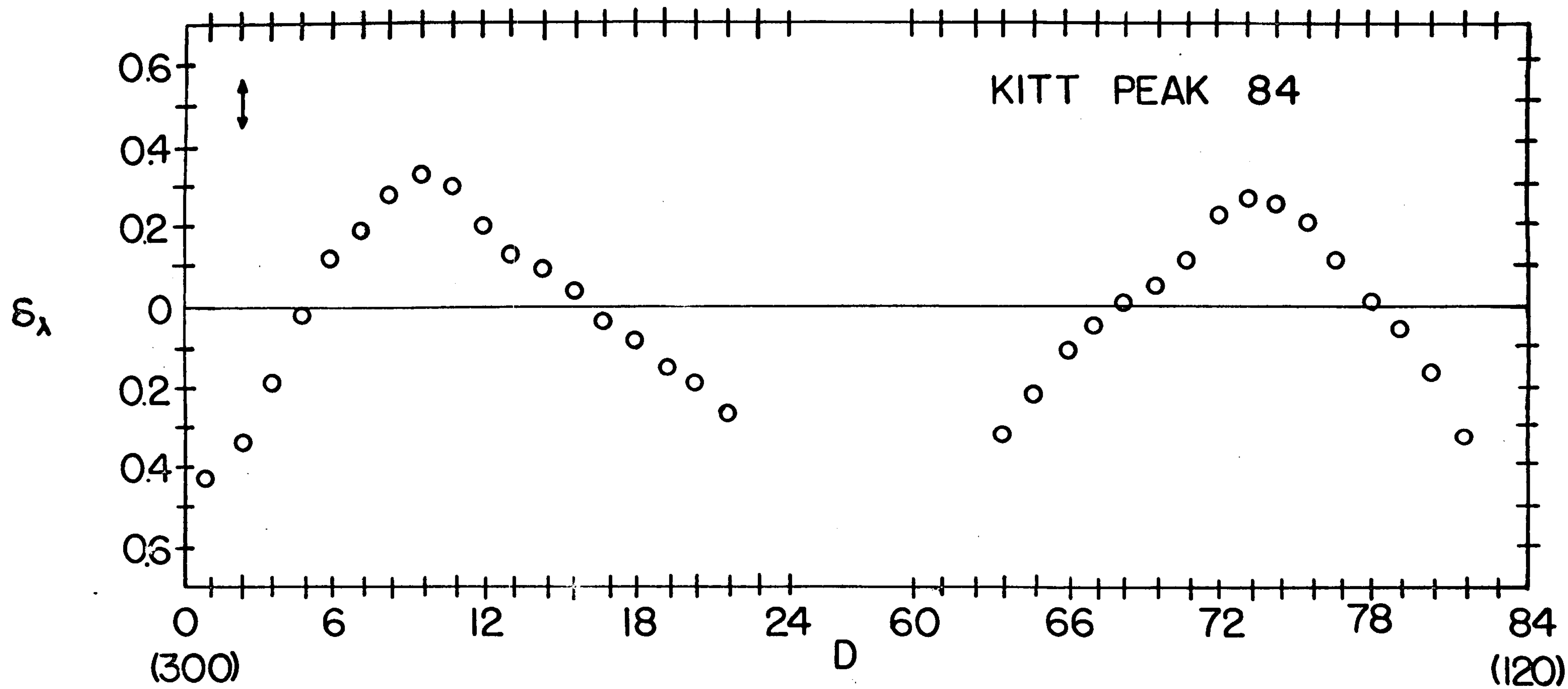
KITT PEAK 84
0.6
0.4
0.2
0
0.2
0.4
0.6
δ_λ
0
6
12
18
24
60
66
72
78
84
(300)
D
(120)

Plot 12

BIBLIOGRAPHY

Johnson, H. 1965, Ap.J., 141, 169.

Kingslake, R. 1926, Trans. Opt. Soc., 28, 1.

__________. 1925, ibid., 27, 94.

Kopal, Z. 1963, Annual Sum. Report, University of Manchester, No. 3, 3.

Mertz, L. 1963, J. Opt. Soc. Amer., 53, (ad. for Block Assoc.).

Saunders, J. B. 1964, J. Res. NBS., 68C, 155.

__________. 1961, ibid., 65B, 239.

__________. 1964, A.J., 69, 449.

__________. 1957a, J. Res. NBS., 58, 21.

__________. 1957b, ibid., 58, 27.

__________. 1963, ibid., 67C, 307.

Strong, J. 1958, Concepts of Classical Optics. (London: W. H. Freeman & Co.), p. 394.

Twiss, R. Q. 1964, Space Physics and Radio Astronomy, ed. by H. Messel and S. T. Butler (London: Macmillan & Co., Ltd.), p. 42.